

2

AFWAL-TR-83-3002

**THERMAL CONDUCTIVITIES AND DIFFUSIVITIES  
OF GRAPHITE-EPOXY COMPOSITES**

Lit S. Han and William F. Boyce

Department of Mechanical Engineering

The Ohio State University, Columbus, Ohio

February 1983



AD A 128 774

Report for period January 1982 - December 1982

Approved for public release; distribution unlimited

DTIC FILE COPY

DTIC  
S MAY 31 1983 D  
H

FLIGHT DYNAMICS LABORATORY  
AIR FORCE WRIGHT AERONAUTICAL LABORATORIES  
AIR FORCE SYSTEMS COMMAND  
WRIGHT-PATTERSON AIR FORCE BASE, OHIO 45433

83 05 31 143

NOTICE

When Government drawings, specifications, or other data are used for any purpose other than in connection with a definitely related Government procurement operation, the United States Government thereby incurs no responsibility nor any obligation whatsoever; and the fact that the government may have formulated, furnished, or in any way supplied the said drawings, specifications, or other data, is not to be regarded by implication or otherwise as in any manner licensing the holder or any other person or corporation, or conveying any rights or permission to manufacture use, or sell any patented invention that may in any way be related thereto.

This report has been reviewed by the Office of Public Affairs (ASD/PA) and is releasable to the National Technical Information Service (NTIS). At NTIS, it will be available to the general public, including foreign nations.

This technical report has been reviewed and is approved for publication.

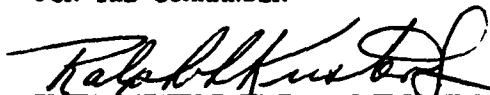


NELSON D. WOLF  
Project Engineer  
Design & Analysis Methods Group



FREDERICK A. PICCHIONI, Lt Col, USAF  
Chf, Analysis & Optimization Branch

FOR THE COMMANDER



RALPH L. KUSTER, JR., Col, USAF  
Chief, Structures & Dynamics Div.

"If your address has changed, if you wish to be removed from our mailing list, or if the addressee is no longer employed by your organization please notify AFWAL/FIBRA, W-PAFB, OH 45433 to help us maintain a current mailing list".

Copies of this report should not be returned unless return is required by security considerations, contractual obligations, or notice on a specific document.

Unclassified

SECURITY CLASSIFICATION OF THIS PAGE (When Data Entered)

REPORT DOCUMENTATION PAGE		READ INSTRUCTIONS BEFORE COMPLETING FORM
1. REPORT NUMBER AFWAL-TR-83-3002	2. GOVT ACCESSION NO. AD-A128774	3. RECIPIENT'S CATALOG NUMBER
4. TITLE (and Subtitle) THERMAL CONDUCTIVITIES AND DIFFUSIVITIES OF GRAPHITE-EPOXY COMPOSITES		5. TYPE OF REPORT & PERIOD COVERED Final Jan. 2, 1982 - Dec. 31, 1982
		6. PERFORMING ORG. REPORT NUMBER 761108/711129
7. AUTHOR(s) Lit S. Han and William F. Boyce		8. CONTRACT OR GRANT NUMBER(s) F33615 - 79 - C- 3030
9. PERFORMING ORGANIZATION NAME AND ADDRESS Mechanical Engineering Department, The Ohio State University, 206 West 18th Avenue, Columbus, Ohio 43210		10. PROGRAM ELEMENT, PROJECT, TASK AREA & WORK UNIT NUMBERS 62201F 24010254
11. CONTROLLING OFFICE NAME AND ADDRESS Flight Dynamics Laboratory (AFWAL/FIBR) AF Wright Aeronautical Laboratories, AFSC Wright-Patterson Air Force Base, Ohio 45433		12. REPORT DATE February 1983
		13. NUMBER OF PAGES 87
14. MONITORING AGENCY NAME & ADDRESS (if different from Controlling Office)		15. SECURITY CLASS. (of this report) Unclassified
		15a. DECLASSIFICATION/DOWNGRADING SCHEDULE
16. DISTRIBUTION STATEMENT (of this Report) Approved for public release; distribution unlimited		
17. DISTRIBUTION STATEMENT (of the abstract entered in Block 20, if different from Report)		
18. SUPPLEMENTARY NOTES		
19. KEY WORDS (Continue on reverse side if necessary; and identify by block number) Carbon, graphite, fiber, epoxy, resin, thermal conductivity, thermal diffusivity		
20. ABSTRACT (Continue on reverse side if necessary and identify by block number) Transient heat conduction experiments were performed on graphite-epoxy composites with fibers oriented uni-directionally in the matrix. With the fiber axis arranged parallel or transverse to the heat flow direction, effective thermal conductivities and diffusivities in the three orthogonal directions were obtained. Also determined in this work were the isotropic conductivity and diffusivity for the epoxy resin (Fibrite No. 934) as 0.136 BTU/hr-°F-ft. and $8.5 \times 10^{-7}$ ft <sup>2</sup> /sec, respectively. (continued)		

Block 20 — Abstract — Continued

A value of  $k = 6.0 \text{ BTU/hr-}^{\circ}\text{F-ft}$  for carbon fibers (Hercules 3501-5A) in the axial direction was deduced. For the conductivity transverse to the fibers, a value of  $2.4 \text{ BTU/hr-}^{\circ}\text{F-ft}$  was obtained from the measured effective transverse conductivity values. The thermal capacities ( $\rho C$ ) for the carbon fibers and resin used in this study were determined as 48.2 and 44.4  $\text{BTU/ft}^3\text{-}^{\circ}\text{F}$ , respectively.

DATE  
COPY  
INSTRUMENTS

Accession For	
NTIS GRA&I	<input checked="" type="checkbox"/>
DTIC TAB	<input type="checkbox"/>
Unannounced	<input type="checkbox"/>
Justification	
By	
Distribution/	
Availability Codes	
Dist	Avail and/or Special
A	

## FOREWORD

The contents of this report are a result of a research program initiated under Project 2401, Structural Mechanics, Task 240102, Design Analysis Methods for Aerospace Vehicle Structures, Work Unit 24010254, Heat Transfer in Composite Materials. The report was prepared by the Mechanical Engineering Department, The Ohio State University, 206 West 18th Avenue, Columbus, Ohio 43210, in partial fulfillment of the requirements under Contract F33615-79-C-3030. The contract was administered under the direction of Mr. Nelson Wolf and Lt. S. Kay Bryan, AFWAL/FIBRA, Wright-Patterson Air Force Base. Their support and indulgence are appreciated by the authors of this report.

The composite test specimens used in this study were fabricated under Mr. Robert Achard's supervision in the Composites Fabrication Facility of the Flight Dynamics Laboratory. His contribution was invaluable and is hereby acknowledged. Additionally, the authors appreciate the help of Dr. James Allen, Fibrite Corp., in donating resin test specimens to our research efforts.

TABLE OF CONTENTS

SECTION	PAGE
I INTRODUCTION	1
II BASIC CONSIDERATIONS	5
III EXPERIMENTAL PROCEDURES AND EQUIPMENT	13
IV ANALYSIS OF TRANSIENT TEMPERATURE DATA	21
V THERMO-PHYSICAL PROPERTIES OF THE CONSTITUENTS	37
VI CONCLUSIONS	43
APPENDIX A: TEMPERATURE DATA AND COMPARISONS WITH PREDICTIONS	45
APPENDIX B: VOLUME-RATIO STUDY	57
APPENDIX C: EQUIPMENT DESCRIPTION	61
BIBLIOGRAPHY	79

v

PRECEDING PAGE BLANK-NOT FILMED

LIST OF TABLES

		PAGE
TABLE		
1	SUMMARY OF EFFECTIVE CONDUCTIVITIES AND EFFECTIVE DIFFUSIVITIES	35
C-1	LIST OF EXPERIMENTAL EQUIPMENT ITEMS	63

## LIST OF ILLUSTRATIONS

FIGURE		PAGE
1	Microscopic End-view of Graphite-epoxy Composite (1500X)	7
2	Schematic Arrangement of Test Apparatus for One-dimensional Heat Conduction	11
3	Test Specimen-block Orientations	15
4	Partially Assembled Test Cell	19
5	Illustration of Least-squares Method for Temperature-profile Matching	24
6	Illustration of Least-squares Error With Best Diffusivity Value	24
7	A Preliminary Assessment of the Diffusivity Value	26
8	Temperature Record for Configuration X Under Constant Heat Flux Condition (Heat Flow Parallel to Fibers)	29
9	Thermal Diffusivity "Variation" for Case XQ	30
10	Least-squares Error Distribution for Case XQ	31
11	Selected Temperature-time Records for Case XQ	33
12	Comparisons of Calculated Temperature Responses Versus Experimental Values, Case XQ	34
A-1	Temperature Profile Matching Results, Configuration X, Constant Heat Flux (XQ)	47
A-2	Temperature Profile Matching Results, Configuration X, Constant Surface Temperature (XT)	48
A-3	Temperature Profile Matching Results, Configuration Y, Constant Heat Flux (YQ1)	49



LIST OF ILLUSTRATIONS (Continued)

FIGURE		PAGE
A-4	Temperature Profile Matching Results, Configuration Y, Constant Surface Temperature (YT1)	50
A-5	Temperature Profile Matching Results, Configuration Y, Constant Heat Flux (YQ2)	51
A-6	Temperature Profile Matching Results, Configuration Y, Constant Surface Temperature (YT2)	52
A-7	Temperature Profile Matching Results, Configuration Z, Constant Heat Flux (ZQ)	53
A-8	Temperature Profile Matching Results, Configuration Z, Constant Surface Temperature (ZT)	54
A-9	Temperature Profile Matching Results, Resin Specimen, Constant Heat Flux (MQ)	55
A-10	Temperature Profile Matching Results, Resin Specimen, Constant Surface Temperature (MT)	56
B-1	Fiber-diameter Population Distribution	60
C-1	Schematic of Experimental Arrangement for Constant Surface Temperature Test	64
C-2	Assembly of Experimental Equipment	65
C-3	Schematic of Experimental Arrangement for Constant Heat Flux Test	68

## NOMENCLATURE

C	specific heat, BTU/lbm-°F.
E	least-squares error, Equation (5), p. 21
k	effective thermal conductivity of composite, BTU/(hr-°F-ft)
T	temperature, °F.
t	time, hour or second
v	volume fraction
x, y, z	orthogonal coordinate; x refers to the heat flow direction, Figure 3

### Greek Symbols

$\alpha$	effective thermal diffusivity, ft <sup>2</sup> /sec
$\rho$	density, lbm/ft <sup>3</sup>

### Subscripts

f	refers to fiber
m	refers to resin matrix
a	along fiber axis
t	transverse to fiber axis

# I

## INTRODUCTION

Among the composite materials, those with fibers in a matrix are the most popular in aerospace structures. There are several reasons for this popularity: one is the high strength and modulus of fiber which contributes significantly to the overall strength of the resulting composite materials. Next is the low thermal expansion of these fibers which manifests itself in the resulting dimensional stability of structures so formed. Furthermore, with the advent of pre-impregnated (prepreg) tapes, formability into various shapes is greatly enhanced. Thus, the increased use of fibrous composites is coupled with lower cost; their expanding applications from aerospace to other adaptations are an indication of their potential role as a candidate material for many applications. Composites, as a new class of materials, have emerged to the full status of an engineering material.

Research efforts in the past have chiefly focused in the mechanical aspects of composites--manufacturing processes and attendant strength, etc. Recent potential applications in which thermal considerations have become a crucial factor point the need for better tools in

analyzing the thermal performance of composite materials in general and fibrous composites in particular under various heat loading conditions. As in the case of research into the mechanical aspects of composite materials, investigations with regard to the thermal aspects proceeded along several avenues. In specific industrial applications, once a composite structure had been designed or fabricated, basic thermal performance parameters--such as the apparent thermal conductivity and a few others--were usually obtained in situ. The resulting data were only specifically addressed to that composite material studied. Data obtained on such an ad hoc basis, scattered in various industrial laboratories, were not amenable to overall coordination in terms of basic correlations between the geometrical dispersion pattern of fibers in matrix, the constituent conductivities, and the apparent thermal conductivity.

Parallel to the above-mentioned type of measurements for their specific needs, basic investigations of heat conduction in composite media have been proceeding in the past decade. Within this framework of basic study, two approaches were pursued: (1) one was to devise methods of calculation of the temperature distribution in composites with simplified dispersion patterns and for shapes of simplified geometries. Inherent in this approach of analysis was that the thermal physical properties of the constituents in a composite medium were known a priori. This type of investigation was exemplified by the work of Horvay, et al. [1], who addressed the problem of transient heat flow in the plane of laminates for a layered composite. Later on, Manaker and Horvay [2] extended the original analysis to problems with various

heating boundary conditions. These were but a small sample of a good number of publications along this approach. As important and elegant were these investigations, the needs of design engineering in estimating thermal conduction in composites were not fulfilled; for want of the thermal physical properties of the constituents; for lack of a correlation between the input parameters (the thermal properties of the constituents and the patterns of dispersion); and for need of the overall thermal performance. (ii) The second approach was to model a composite medium as a single-phase body which has thermal characteristics, in particular thermal conductivities, reflective of those of the ingredients. In other words, the principal thermal properties were expressed by an effective thermal conductivity, which may be directionally dependent, and an effective thermal inertia. These effective values were manifestations of those of the constituent materials, in the case of a fibrous material, the fibers and the matrix material. The relationships between the constituents and an effective medium as a model replacement were the main focus of many research efforts. The establishment of such a relationship was a principal objective which resulted in a publication by Han and Cosner [3].

Since the previously described efforts of both types were predicated on a foreknowledge of the basic thermal properties of the constituents, a natural question arose as to the availability of the information, in particular, relative to carbon fibers and resin as a matrix material. Data of this sort were meager in the literature. Consequently, a purpose of this experimental investigation within the framework of

a larger effort to develop heat transfer methods for composite material was to provide information needed to bridge the gap. A secondary purpose of this experimental investigation was to evolve a reliable, inexpensive experimental procedure—by way of demonstration with carbon/epoxy composites so that other composites may be similarly treated.

With these two objectives in mind, the geometrical dispersion pattern of fibers in a binding matrix was made as simple as possible and more importantly to conform with the dispersion pattern analyzed in [3]. Hence, a carbon/epoxy composite with a uni-directional fiber orientation was used in this study.

## II

### BASIC CONSIDERATIONS

In an isotropic medium, heat conduction is governed by three physical properties of the medium: thermal conductivity  $k$ , density  $\rho$ , and specific heat  $C$ . The last two are invariably joined together as a product term. From these three parameters, the thermal diffusivity  $\alpha$  is defined as:

$$\alpha = k/(\rho C)$$

For steady-state conduction, the thermal conductivity  $k$  alone determines the entire temperature distribution throughout the body; whereas for transient heat flows, the thermal diffusivity coefficient  $\alpha$  becomes equally important. Conceptually, it denotes the ability of diffusing, or passing on by virtue of conduction, that energy originating at the input site in a material body in question.

It is of importance to note that the physical properties  $\rho$  and  $C$  are scalars and the thermal conductivity  $k$  may be directionally dependent, in which case the term orthotropic is used. For composites consisting of uni-directional fibers in a body of the binding matrix, transfer of heat encounters different resistances depending on the direction of heat propagation. Hence, in composites, there are, generally speaking,

three effective thermal conductivities: one for heat conduction parallel to the fiber axis, and the other two for transverse heat flows in the remaining directions. Assuming (in fact, true) that carbon fibers are more conductive than the matrix materials, conduction of heat in the direction of the fiber axis therefore constitutes a series of parallel flow circuits with the flow along the fibers as a short circuit. High effective conductivities are a consequence. For heat conduction transverse to the fiber axis, the high-conductivity fibers become local inclusions embedded in the low-conductivity matrix material; therefore, a lower effective conductivity is expected. Aside from these effects, carbon fibers and, for that matter, most synthetic fibers, exhibit different conductivities when heat conduction occurs parallel versus transverse to them. That is, due to the manner in which the polymers are aligned with the fiber axis, a higher conductivity results when heat is transferred parallel to the fiber rather than normal to it.

A cross-sectional view of a sample of the carbon/epoxy composite used in this study is shown in Figure 1 indicating the discrete fibers (more properly, bundles of fibers) in a resin matrix. The two groups of fibers are separated by a wide channel consisting of the matrix material only; the appearance of a canal-like structure is a result of two prepreg tapes interfacing each other. Within each tape, there is, however, an orderly identifiable, geometrical pattern. The cross-sectional view of Figure 1 was obtained by mounting, polishing and then microscopically photographing an end view of the composite specimen. A further enlargement of the microscopic image, 2100 times the original size, was then used in order



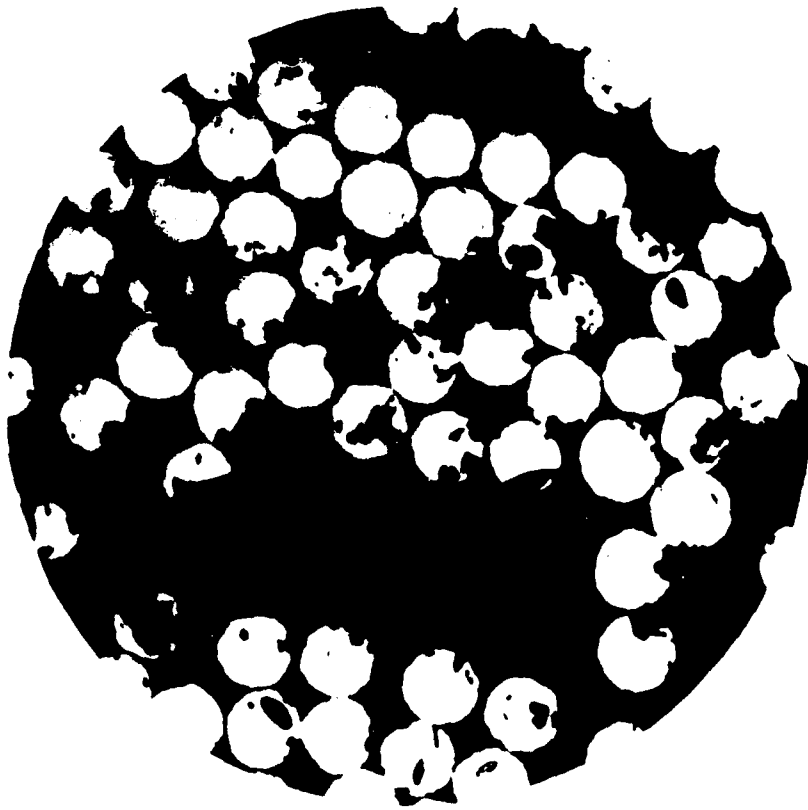


Figure 1. Microscopic End-view of Graphite-epoxy Composite (1500 X).

to determine the volume ratio of the composite, i.e., the ratio of the fiber volume to the total volume; details were documented in Appendix B.

1. EXPERIMENT RATIONALE

In principle, the thermal characteristic of a composite consisting of uni-directional fibers in a matrix, are completely defined once the thermal properties of the constituents and the geometrical dispersion pattern are known. Indeed, such was the basic tenet in a previous effort [3]. However, direct measurements of the properties of the elementary materials entail a great deal of difficulties, especially for the fibers because of the directional dependence. In this experimental investigation, a transient heat conduction technique was used, first to determine the effective thermal diffusivities in the three principal directions, and then to synthesize the data obtained in order to delineate the thermal-physical properties of the constituents.

Conceptually, the experiment consists of imparting a constant heat flux on one surface of a composite specimen block while the surface opposite to the heating surface was kept at the initial temperature of its specimen block. With the remaining peripheral surfaces insulated against heat losses, one-dimensional heat conduction was thereby achieved, for which the governing differential equation was:

$$\rho C(\partial T/\partial t) = k(\partial^2 T/\partial x^2) \quad (1)$$

where:

$T$  = local temperature of the composite body

$t$  = time

$x$  = coordinate of the heat flow direction

$k$  = effective conductivity for heat flow in the  $x$  direction

$\rho C$  = effective thermal inertia of the composite material

The temperature  $T$  in Equation (1) represents an average value of the fibers and matrix at the location concerned.

Since the product  $(\rho C)$  is composed of scalar quantities of the constituents, its value is a linear combination based on the volume fractions of fibers and matrix material, respectively,

$$(\rho C) = (\rho C)_f v_f + (\rho C)_m v_m \quad (2)$$

where  $v_f$  and  $v_m$  denote the fractions of the fiber volume and matrix volume, respectively, with  $v_f + v_m = 1$  naturally. The subscripts  $f$  and  $m$  refer to the fiber and matrix constituents.

The effective conductivity  $k$  in Equation (1) is related to the thermal conductivities of the two different constituents in terms of a parametric relation,

$$(k/k_m) = F(k_f/k_m, \text{geometry}) . \quad (3)$$

For heat conduction along the axial direction of uni-directional fibers, Equation (3) assumes a particularly simple form:

$$k_a = v_f k_{fa} + v_m k_m . \quad (4)$$

For heat conduction transverse to the uni-directional fibers, the relationships expressed by Equation (3) are rather involved and have been thoroughly analyzed in an earlier study [3]. Equations (1), (2), and (3) plus required boundary conditions constitute the basis for experiments from which temperature data are to be analyzed in order to obtain the basic thermo-physical property values of the constituents.

## 2. METHOD OF EXPERIMENTAL DATA ANALYSIS

Consider a one-dimensional heat conduction experiment for which the physical arrangement is shown in Figure 2. Two identical test specimen blocks are located symmetrically on both sides of a centrally located heating plate assembly. For each specimen block, one surface is in contact with a cooling plate which keeps the specimen's surface temperature at a constant value.

During a transient heat conduction experiment, the central heater is activated, sending one-half of the electric heat input to the specimen block. Symmetry of the physical arrangement assures this even heat division. By monitoring the two surface temperatures, one on the heating surface and the other on the cooling surface, and at least one more temperature in an interior location of the specimen block, there are obtained three temperature-time histories at three points, illustrated as points A, B, and C in Figure 2. From the well-established theory of heat conduction, the C constitutes the boundary conditions in solving Equation (1). The solution for point B is uniquely determined if the

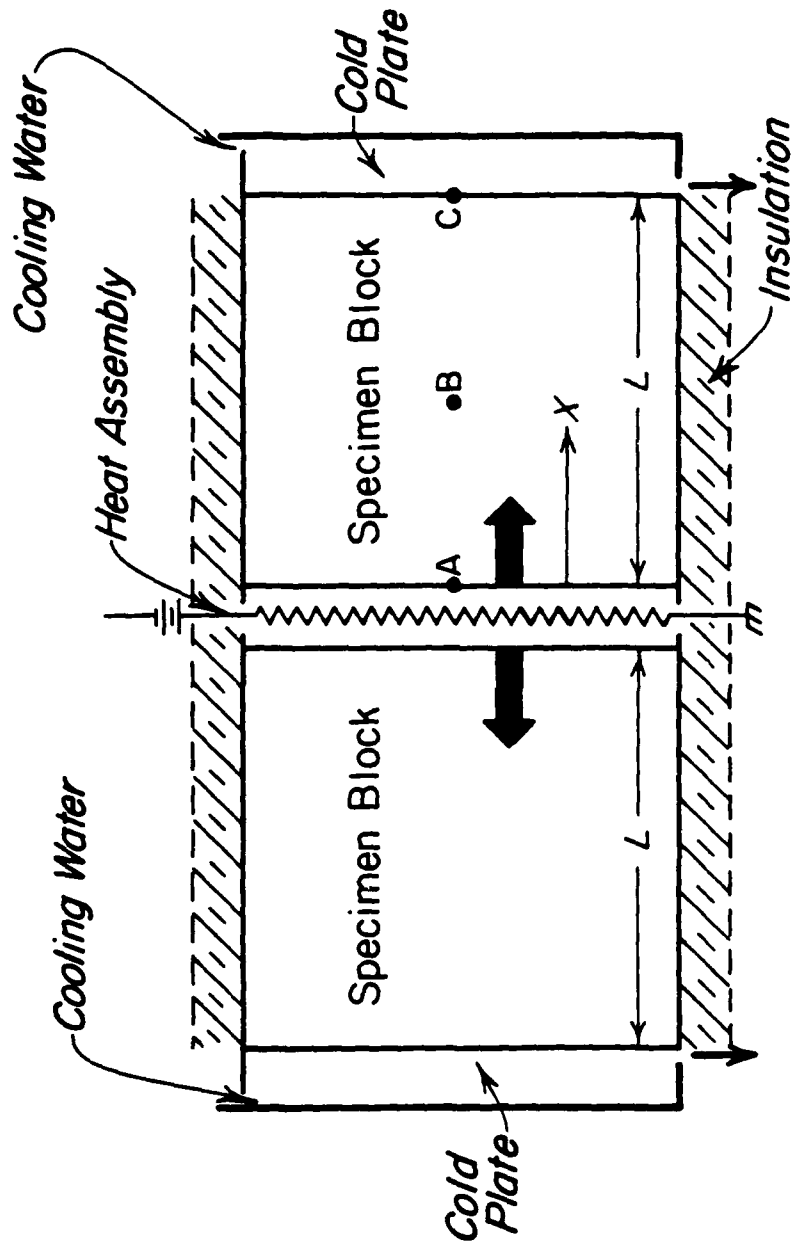


Figure 2. Schematic Arrangement of Test Apparatus for One-Dimensional Heat Conduction.

thermal diffusivity value (effectively speaking)  $\alpha$  is known. Employing this procedure in reverse, the recorded temperature-time variation at point B therefore determines the effective diffusivity value for the composite in the experiment and in the direction of the heat flow.

Furthermore, when steady state heat conduction is reached resulting in a linear temperature distribution along the heat path A-B-C, an effective thermal conductivity can be determined based on the steady-state temperature data and the known heat flow through the specimen block. Thus, in a single transient experiment, it is possible to determine the values of  $k$  and  $\alpha$ , from which an effective thermal inertia ( $\rho C$ ) can be extracted.

By preparing specimen blocks so that the uni-directional fibers are either aligned with, or transverse to the heat flow direction, directional effective thermal conductivities can be determined. Similarly, by using specimen blocks with the matrix material alone, the basic thermal conductivity  $k_m$  and the thermal inertia  $(\rho C)_m$  can be obtained.

### III

#### EXPERIMENTAL PROCEDURE AND EQUIPMENT

##### 1. TEST SPECIMENS

A number of graphite-epoxy slabs with graphite fibers oriented uni-directionally and of dimensions 6 x 6 inches square, 0.5 inch thick, were used in this experimental study. The composite specimens were prepared by the Flight Dynamics Laboratory, Composites Facility, under the supervision of Mr. Robert Achard; they were fabricated by a standard process starting with prepreg tapes which were supplied by Hercules, Inc. The manufacturer's identifications for the resin and fibers were 3501-5A and AS-1, respectively; and according to the supplier, the fiber content in the prepreg form was 42(+3) percent by weight and the ply (tape) thickness was 0.0052 (+0.0004) inches. However, a direct count using a photo-image process conducted in this study, as outlined in Appendix B, determined that the volume ratio for the fibers was equal to 59.7 percent.

Also used in this experimental study were half-inch thick slabs of pure resin (934) supplied by Fibrite Corp. The resin in these slabs was of essentially the same chemical composition as that in the composite slab.

## 2. TEST CELL

The test cell consisted of three basic elements: a centrally located heater assembly and two cooling plates. Between the heater assembly and the cooling plates, two identically constructed specimen blocks were inserted so that symmetry of the geometrical arrangement assured that half of the heater input traveled through one test block. A schematic diagram has been presented in Figure 2.

The heater assembly was composed of two aluminum surface sheets, either 6 x 6 square or 3 x 6 rectangle, and 0.03 inches thick; the two surface sheets encapsulated a foil heater of the same dimensions as those of the surface sheets. The heater of 3 x 6 inches square was used in conjunction with configuration X for the heat flow experiments along the fiber axis direction. This configuration and the other two are illustrated in Figure 3. The heater of 6 x 6 inches rectangle was used for configurations Y. The foil heater was a thin film-type containing electric-conducting films arranged in a serpentine pattern and insulated by a Kapton coating. The overall thickness of the film heater was 0.007 inches and the heaters had a maximum operating temperature of 350°F. They were supplied by Electro-Film Co., Los Angeles, California.

The cooling plates located at the two ends of the test apparatus were 6 x 6 square, made of two aluminum surface sheets enclosing a series of zigzag channels through which cooling water was passed. The temperature of the cooling water was maintained by re-circulating it to and from an external tank with ice as the heat sink.



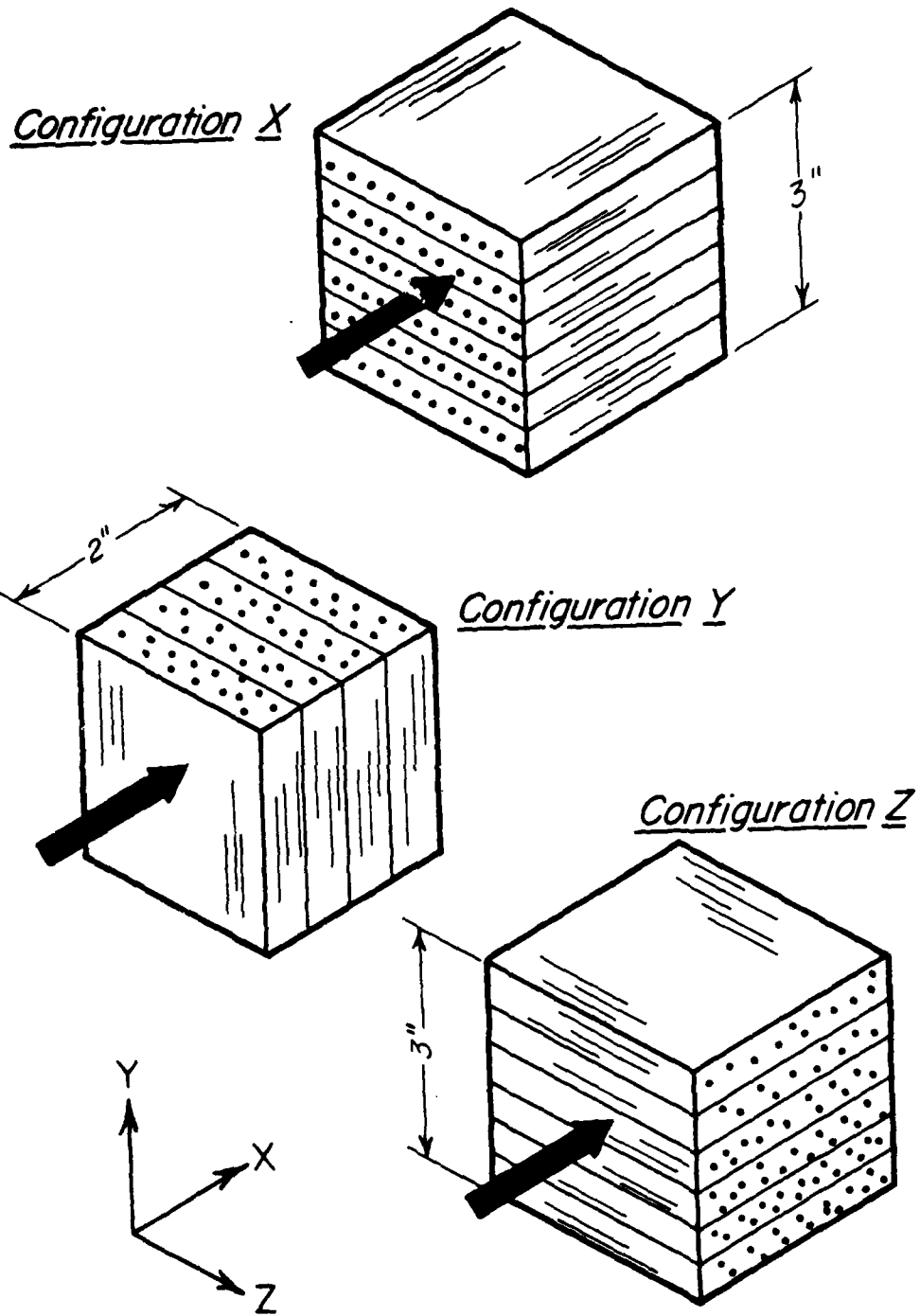


Figure 3. Test Specimen Block Orientations.

### 3. TEST SPECIMEN ORIENTATION

For determining the thermal properties of the carbon/epoxy composites, a number of identical specimen slabs were stacked upon each other to form or simulate a single test block. Three different arrangements were used resulting in three different orientations of the carbon fibers relative to the heat flow direction. They are identified in Figure 3 as configurations X, Y, and Z.

In order to evaluate the thermal properties of the composites when heat flow travels along the fiber axis, configuration X was used. For each of the two identical test blocks, six slabs were used to form a block of 6 x 6 x 3 inches as shown in Figure 3. The heating area was therefore 3 x 6 and faced a heating plate of the same dimension.

On each of the surfaces of the heater assembly and the cooling plate, three thermocouples were centrally located to monitor the surface temperature variations of the test block, corresponding to locations A and C in Figure 2. With test block surfaces machined flat and with a thermal grease (Thermal Paste No. OT-201, Omega Engineering, Inc., Stamford, Connecticut) at the interfaces, the measured temperatures were equal to those of the specimen block surfaces. For configurations X and Z, heat conduction was parallel to the plane of the slabs, thermal grease was not used at the inter-slab surface, otherwise the heat flow paths through the interfacial thermal grease would constitute a heat flow short-circuit. However, for configuration Y, where the heat paths were normal to the slabs, thermal grease was used at the interfaces so that the entire assembly of slabs became a single thermal block.

For monitoring the interior temperature-time variations of the simulated specimen block of configuration X, three thermocouples were embedded on the center line of the middle slab. They were located in the middle of the heat flow path and at 1 inch, respectively, from the hot and cold ends. With  $x=0$  and 6 denoting the positions of the hot and cold surfaces in that order, the interior thermocouples were located at  $x=1, 3,$  and 5 inches from the surfaces.

For configuration Y in Figure 3, arranged to determine the thermal conductivity transverse to the fibers, four specimen slabs (on each side) were thermally joined to form a single block. A heater assembly of 6 x 6 was used, and interface thermocouples at  $x = 0.5, 1, 1.5$  inches from the heating surface were centrally located with respect to the slabs to monitor the interior temperature variations.

In order to complete the three principal values of the thermal conductivities, configuration Z, as illustrated in Figure 3, was used to determine the second transverse effective conductivity. For each test block, six slabs were stacked to form a single test block; and, as in configuration X, the heat flow path was confined to the plane of the slabs and no thermal grease was used in the interfaces between slabs. Five interior thermocouples were embedded on the surface of the middle slab; they were at  $x = 1, 2, 3, 4$  and 5 inches from the heating surface and were lined up, right in the middle of the block assembly.

For each of the specimen orientations, two transient heat flow tests were conducted, one with the heater assembly at a constant heat flow condition and the other with the heat input regulated by a controller so that the interface condition simulated a constant temperature

condition. In this way, some degree of corroboration was achieved in the basic thermal data obtained.

Shown in Figure 4 is a partially assembled test apparatus.

4. TEST IDENTIFICATION

For each of the three configurations identified in Figure 3 for the different fiber orientations relative to the heat flow direction, two transient tests were performed, one at a constant heat flux and the other at a constant temperature. The test run identifications follow the designations XQ, XT, YQ, etc. In addition, resin slabs were stacked in configuration Y of Figure 3 and this test run was identified as test M. The following tabulation completes this experimental range.

Test XQ - Heat Flow Parallel to Fibers, Constant Heat Flux

Test XT - Heat Flow Parallel to Fibers, Constant Surface  
Temperature

Test YQ - Heat Flow Transverse to Fibers, Constant Heat  
Flux (also transverse to slabs)

Test YT - Heat Flow Transverse to Fibers, Constant Surface  
Temperature (also transverse to slabs)

Test ZQ - Heat Flow Transverse to Fibers, Constant Heat  
Flux (parallel to slab)

Test ZI - Heat Flow Transverse to Fibers, Constant Surface  
Temperature (parallel to slab)

Test M - Heat Flow through Resin Slabs

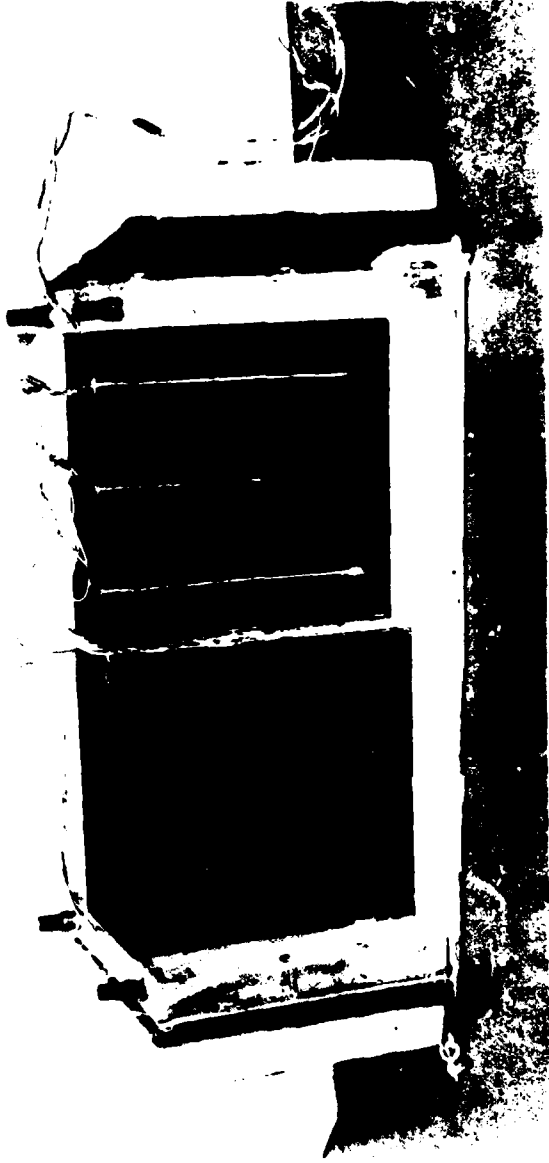


Figure 4. Partially Assembled Test Cell.

#### IV

### ANALYSIS OF TRANSIENT TEMPERATURE DATA

#### 1. TEMPERATURE-PROFILE MATCHING

As outlined in Section II, the method of temperature profile matching was used to analyze and to extract the thermal diffusivities of the composite along the three principal axes of heat flow. Conceptually, the method was based on the fact that the measured temperature-time history in the interior of the composite specimen block (assumed to be a complete solid block) would match exactly with the solution to the one-dimensional heat flow equation, provided that the experimentally recorded surface temperature variations (at the heating surface and the cooling surface) were used as the boundary conditions to the differential equation, and provided that a correct value for the thermal diffusivity was used in the governing equation.

In order to determine the correct effective thermal diffusivity for a particular test orientation, i.e., configurations X, Y, or Z as indicated in Figure 3, the reverse to the above described matching was employed. In other words, the one-dimensional heat conduction equation was solved with the experimentally obtained surface temperature variations as the boundary condition, but with thermal diffusivity value  $\alpha$  in Equation (1) varied so that for each diffusivity value assumed in the solution scheme, there would be a temperature field as a function of

position and time for the interior of the composite body in question. With the interior temperature-time histories experimentally obtained at several stations, it would be therefore possible to decipher which thermal diffusivity value best represents the thermal characteristic of the composite. To simplify the matter, a single point in the interior was chosen. It should not be on one of the two boundary surfaces and not too close to them, for on either one of the two surfaces, the calculated temperatures would be exactly equal to the measured values, which were used as the boundary conditions. A logical choice was, therefore, a point half-way between the heating and cooling surfaces.

In searching for the best thermal diffusivity value, so that the calculated temperature variation (with time) at the midway point best described the experimentally obtained temperature variation, a quantitative criterion had to be established, since it was unreasonable to expect that these two variations would have fallen on top of each other. A least-squares error was therefore chosen as the criterion to judge the best thermal diffusivity value. This method is illustrated by considering three tentative values of the thermal diffusivities  $\alpha_1$ ,  $\alpha_2$ , and  $\alpha_3$ . Their values, in conjunction with the surface boundary conditions, produced three temperature-time history curves for a reference point in the composite. In addition, there was an experimentally recorded temperature variation, which served as the reference to judge the values of the thermal diffusivities. The four temperature variations are illustrated in Figure 5.

According to the method of least squares, an integrated error is defined by the general formulation:

$$E = \sqrt{\left[ \int_0^{t_0} (T_{\text{exp}} - T_{\alpha}) dt \right] / t_0} \quad (5)$$

where:

- $t_0$  = cut-off time, i.e., the end of the transient period
- $T_{\alpha}$  = temperature variation at the reference point from one-dimensional heat conduction equation based on  $\alpha$ .
- $T_{\text{exp}}$  = experimental temperature variation.

Hence, for each  $\alpha$ -value assumed, there was an associated error integral value  $E$  and a functional relationship can be established between them and is illustrated in Figure 6. It follows that the minimum value of  $E$  located the best value for the thermal diffusivity.

## 2. ONE-DIMENSIONAL HEAT CONDUCTION SOLUTION (FINITE-DIFFERENCE)

To solve the one-dimensional heat conduction Equation (1) with the experimentally determined surface temperature variations as the input boundary conditions, it is entirely possible to start with the exact, analytical solution with the effective thermal diffusivity  $\alpha$  as a parameter in the solution expression. However, solutions of this type are usually represented by an infinite series in conjunction with the Duhamel's integrals, which are not easy to evaluate.

Instead of the exact-solution approach, a finite difference method of solving the heat conduction was used. An explicit time-marching technique was adopted, with a stability criterion of:

$$\alpha(\Delta t / \Delta x^2) \leq 0.5 \quad (6)$$



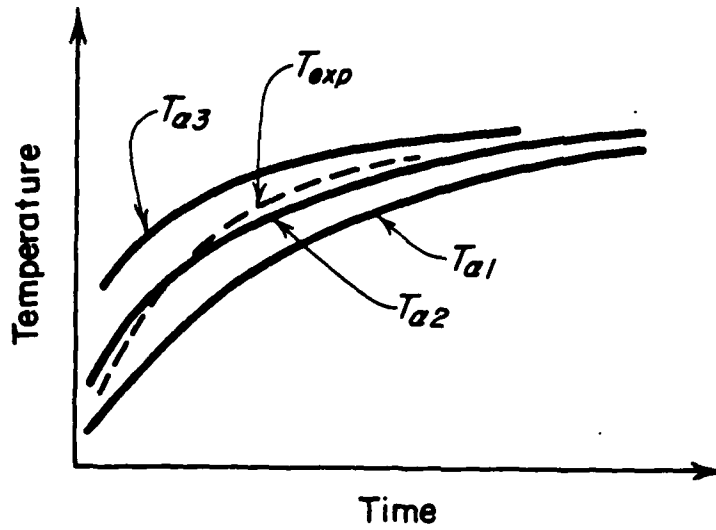


Figure 5. Illustration of Least-squares Method for Temperature-profile Matching.

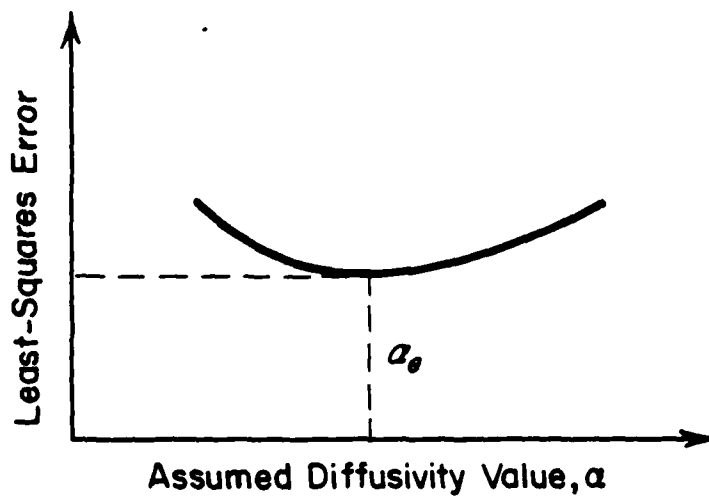


Figure 6. Illustration of Least-squares Error With Best Diffusivity Value.

This rendered the simplest computer routine possible in order to obtain the temperature variations throughout the composite domain. Eleven to fifteen space divisions were used which were judged to have sufficient accuracy in the time-marching scheme.

### 3. PRELIMINARY ESTIMATE OF THERMAL DIFFUSIVITY

In obtaining the finite-difference solutions with various values of the thermal diffusivity, it was deemed desirable to have an approximate idea as to where the range of the value for  $\alpha$  lay. This was accomplished by first interpreting the heat conduction equation in the following form:

$$\alpha = (\partial T / \partial t) / (\partial^2 T / \partial x^2) \quad (7)$$

Thus, at a reference point  $x$  (half-way between the heating and cooling surfaces), the ratio of the time derivative to the space derivative could give an order-of-magnitude estimate of the diffusivity value. In principle, this method would give an exact value; in practice, the errors in obtaining the derivatives from the experimental values were too large to have any credence to the results.

To implement this preliminary assessment, consider three experimentally obtained temperature-time curves at three positions  $x_1$ ,  $x_2$ ,  $x_3$ , equal distance apart from one another, as illustrated in Figure 7. At the reference position  $x_2$ , the time derivative and space derivative are respectively given by simple formulas and their ratio gives the value of the thermal diffusivity at  $x_2$  as:

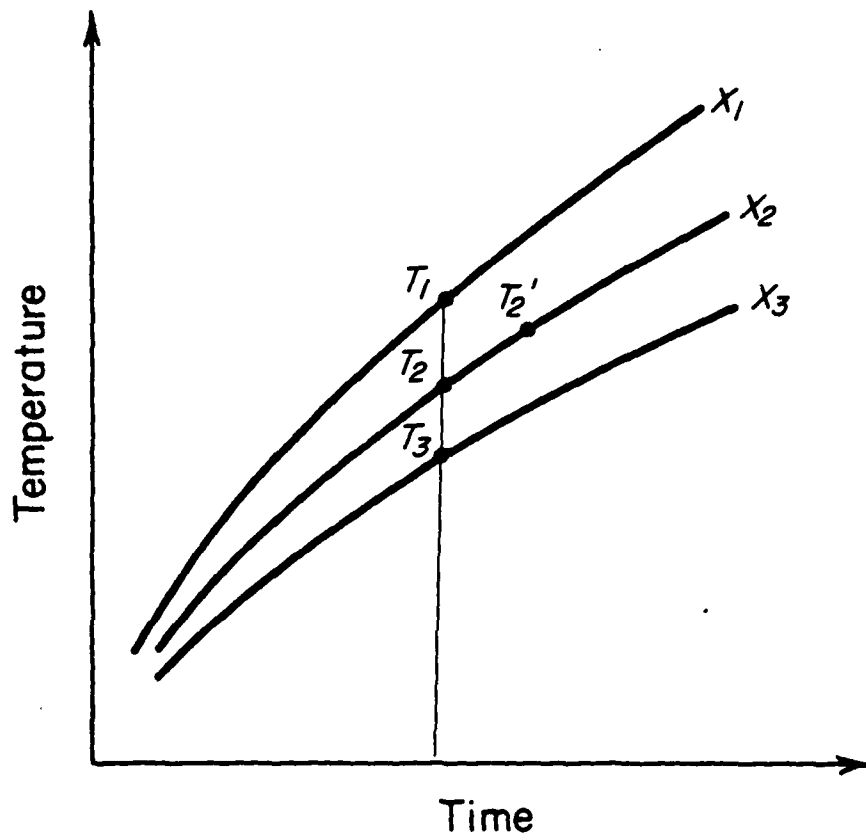


Figure 7. A Preliminary Assessment of the Diffusivity Value.

$$\alpha = [(T_2' - T_2)/(T_1 + T_3 - 2T_2)][(\Delta x)^2/\Delta t] . \quad (8)$$

Evaluation of the right-hand side member offers some practical difficulty; at very small times, these four temperatures are simply too close to one another to give a reasonable resolution; at large times, however, as the temperature field tends toward a steady-state situation, the ratio becomes indeterminate. Only at intermediate times does the above formula give a reasonable indication as to where  $\alpha$  lies approximately. In this way, this method provided a starting point to search for the correct diffusivity value by the method of temperature-profile matching, which will be discussed next.

#### 4. ANALYSIS OF TEMPERATURE RECORD

For all the test runs conducted, the treatment of the temperature-time record was essentially similar. The basic steps are described in this section for test run XQ which refers to configuration X, Figure 3, i.e., heat flow was along the fiber axis and the boundary condition at the heating surface was that of constant heat flux. Naturally, the actual surface temperature variation measured was used as the boundary condition.

By way of describing the experimental results and conditions in detail, other experimental runs were also covered. Cooling water at 51.7°F ( $\pm 0.6^\circ\text{F}$  variation) was used in the cooling plates which brought the entire assembly to an initial temperature of 51.7°F after 5 hours of cooling period. Transient heat flow commenced by turning on the heater switch so that a total of 100 watts ( $\pm 2$  variation) heat input was maintained. Symmetry of the test arrangement assured that a

constant surface flux of 50 watts ( $\pm 1$  variation) was imparted to the specimen surface. Temperatures recorded were those at the heating surface, the cooling surface, and three intermediate points between the two boundaries. The intermediate points, i.e., those thermocouples located inside the composite, were 1, 3, and 5 inches from the heated surface. Figure 8 illustrates the five temperature-time histories obtained from this test run.

The data displayed in Figure 8 were treated as follows: first, a crude estimate of the thermal diffusivity was made based on the formulation in Section 4.3. At a selected time instant, the three temperatures were those at positions of  $x = 1, 3,$  and  $5$  inches, respectively, i.e.,  $\Delta x = (1/6)$  ft.; the temperature-time gradient was obtained by subtracting the two successive measurements of the temperature at  $x = 3$  inches. In this manner, an  $\alpha$ -value was obtained. By repeating the procedure at different time instants, a record of "variation" of thermal diffusivity with time was obtained; this particular run, XQ, is shown in Figure 9. The "variation" of the diffusivity values were of course caused by the inaccuracy inherent in the formulation of Equation (8). However, the record gave an indication as to the limits in which the correct value lay; it was within a lower and upper limit of  $0.25 \times 10^{-5}$  and  $1.5 \times 10^{-5}$  ft<sup>2</sup>/sec. From these limiting values, the finite-difference equation was invoked to determine the error integral E, defined by Equation (5), with the experimentally determined temperatures at  $x = 3$  inches as the reference temperatures. By varying the diffusivity value, various error integrals were obtained, and the minimum value of the latter was found at a diffusivity value of  $\alpha = 3.3 \times 10^{-5}$  ft<sup>2</sup>/sec. Figure 10

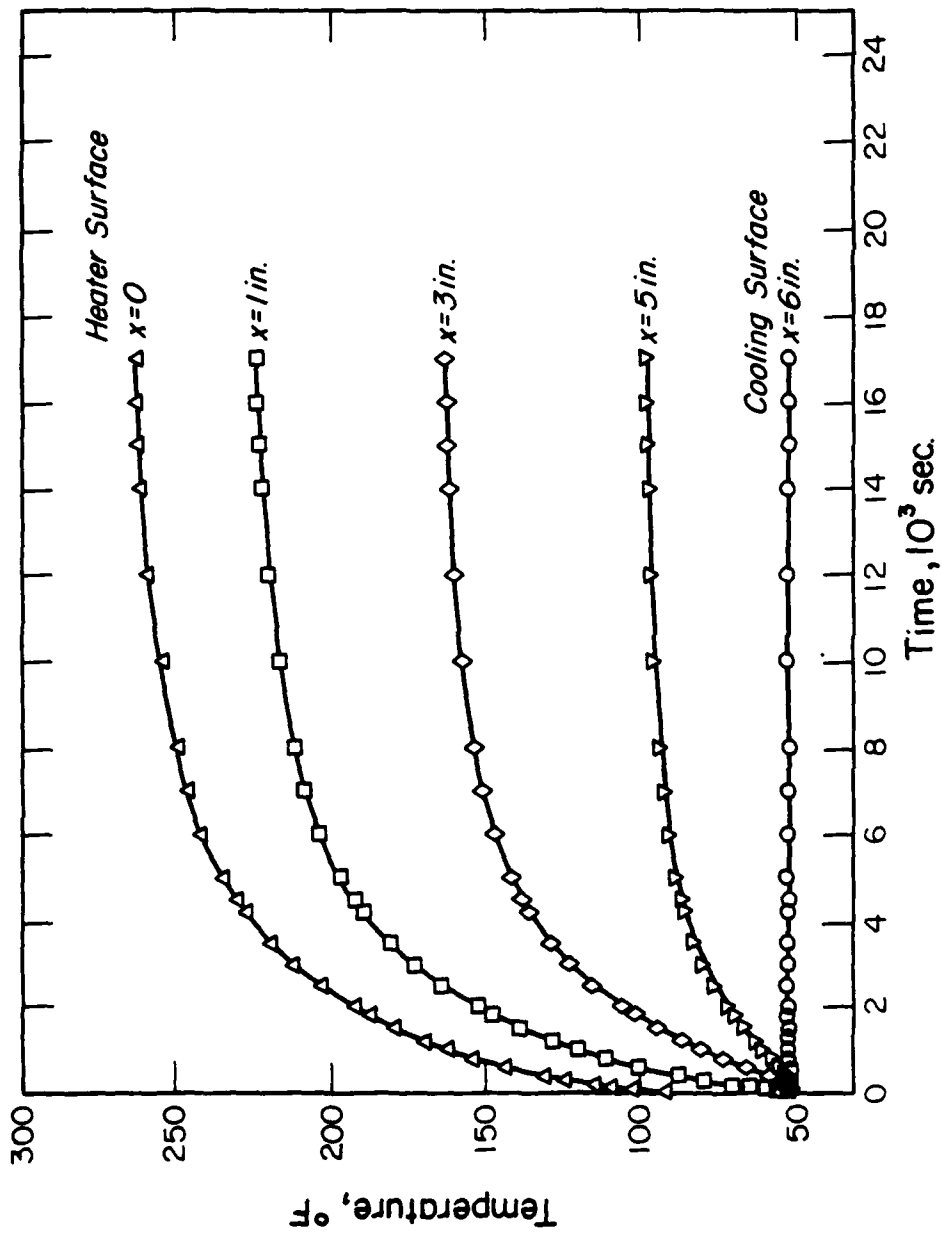


Figure 8. Temperature Record for Configuration X Under Constant Heat Flux Condition (Heat Flow Parallel to Fibers).

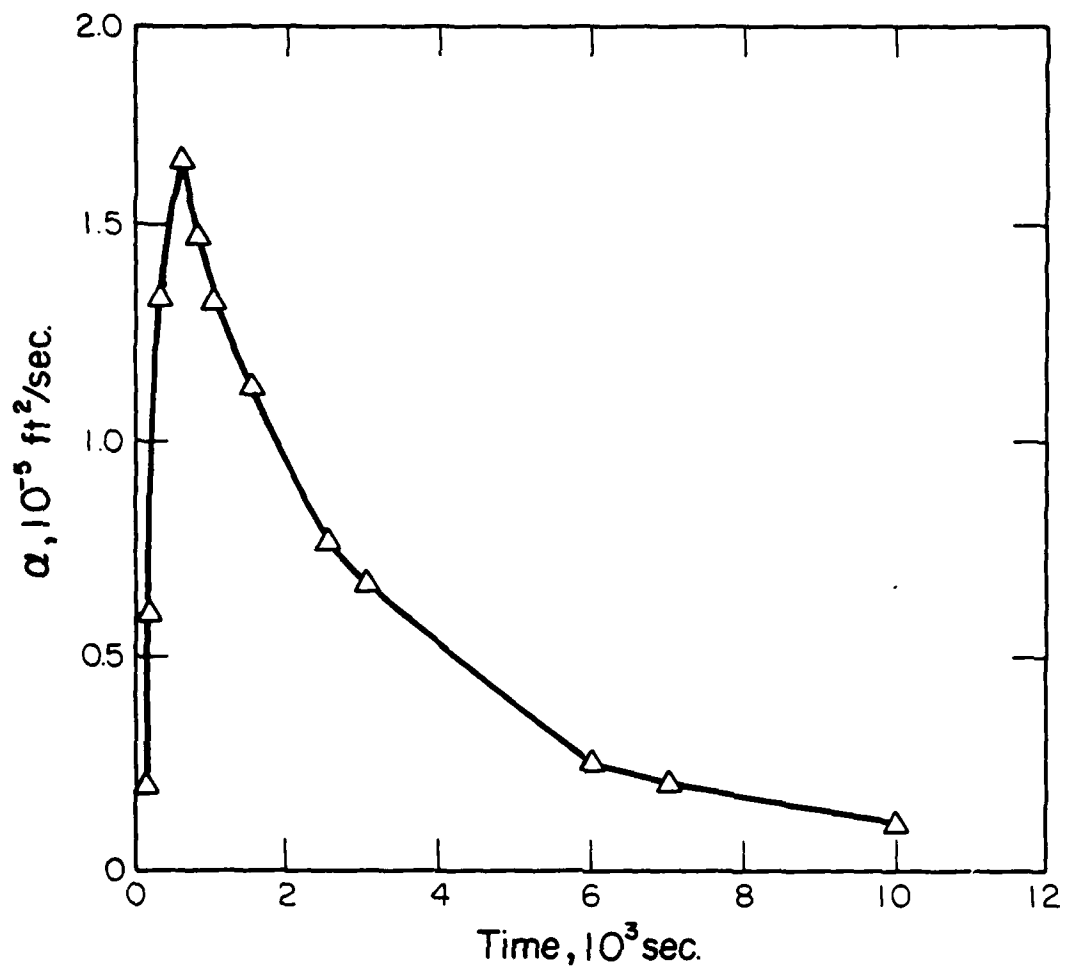


Figure 9. Thermal Diffusivity "Variation" for Case XQ.

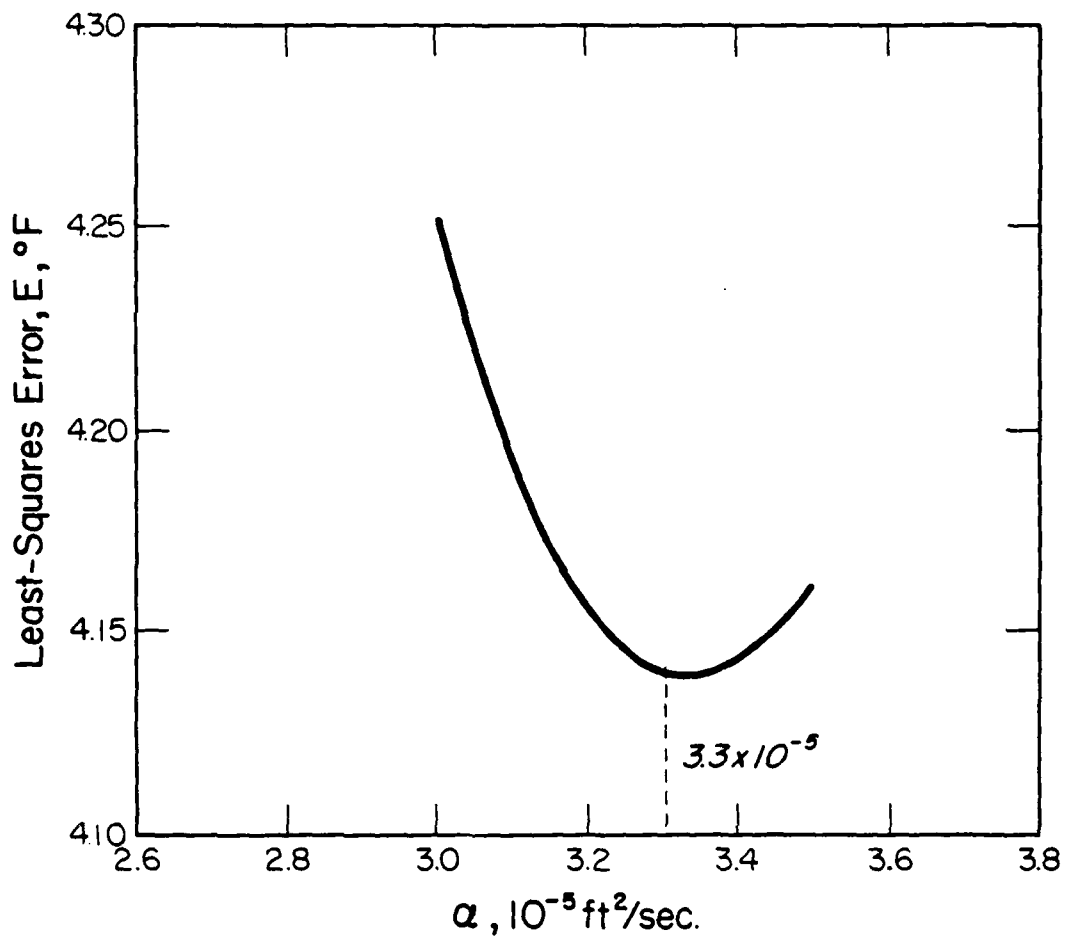


Figure 10. Least Squares Error Distribution for Case XQ.



shows the computed distribution of the error integral E at various assumed values of  $\alpha$ . For test run XQ, a value of  $3.3 \times 10^{-5}$  for effective thermal diffusivity in the direction along the fiber axis was obtained.

At the conclusion of the transient period, a steady-state temperature distribution was obtained, which was used to calculate the effective thermal conductivity along the fiber-axis direction. Such a steady-state temperature record was indicated in Figure 11, which also showed the temperatures at selected time instants. The effective thermal conductivity turned out to be 3.63 BTU/hr-°F-ft.

Having obtained the effective diffusivity value, one would like to compare it with the calculated temperatures from the one-dimensional differential Equation (1), using the effective diffusivity of  $3.3 \times 10^{-5}$  ft<sup>2</sup>/sec. For test run XQ, three temperature records at  $x = 1, 3,$  and 5 inches, respectively, were available; their temperature variations, together with the calculated variations, are shown in Figure 12. The calculated values at  $x = 1$  inch were above the experimental while those at  $x = 5$  inches were below the measured data. For the reference position of  $x = 3$  inches, agreement appears satisfactory.

The individual diffusivity and conductivity values from all test runs were extracted in a similar fashion and were summarized in Table 1. A noteworthy feature of the data was the fact that the effective thermal conductivity for heat flow parallel to the fiber axis was one order of magnitude above the corresponding value for heat flow transverse to the fiber axis.

The transient temperature records for all test runs as well as comparisons of the predicted values at the interior points based on the

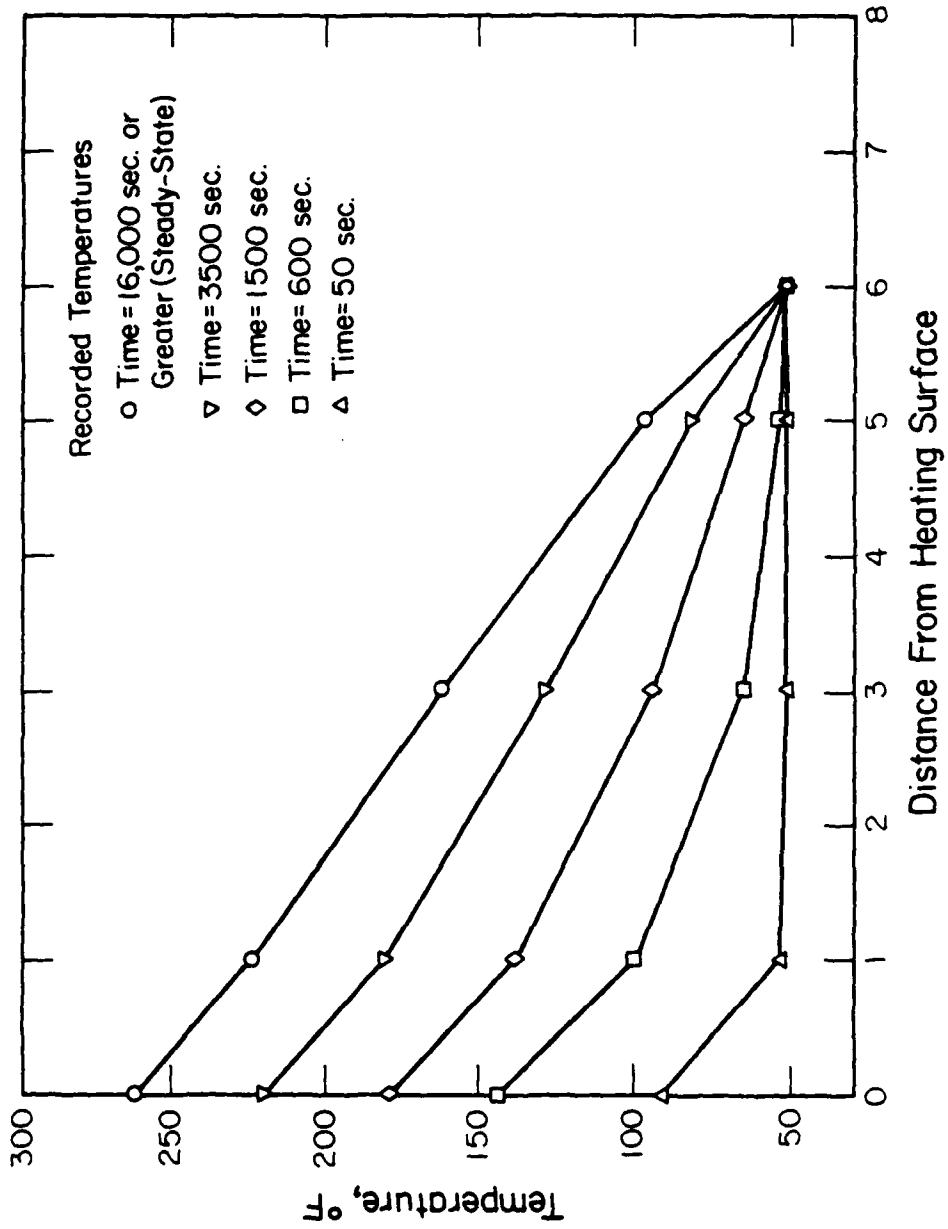


Figure 11. Selected Temperature-time Records for Case XQ.

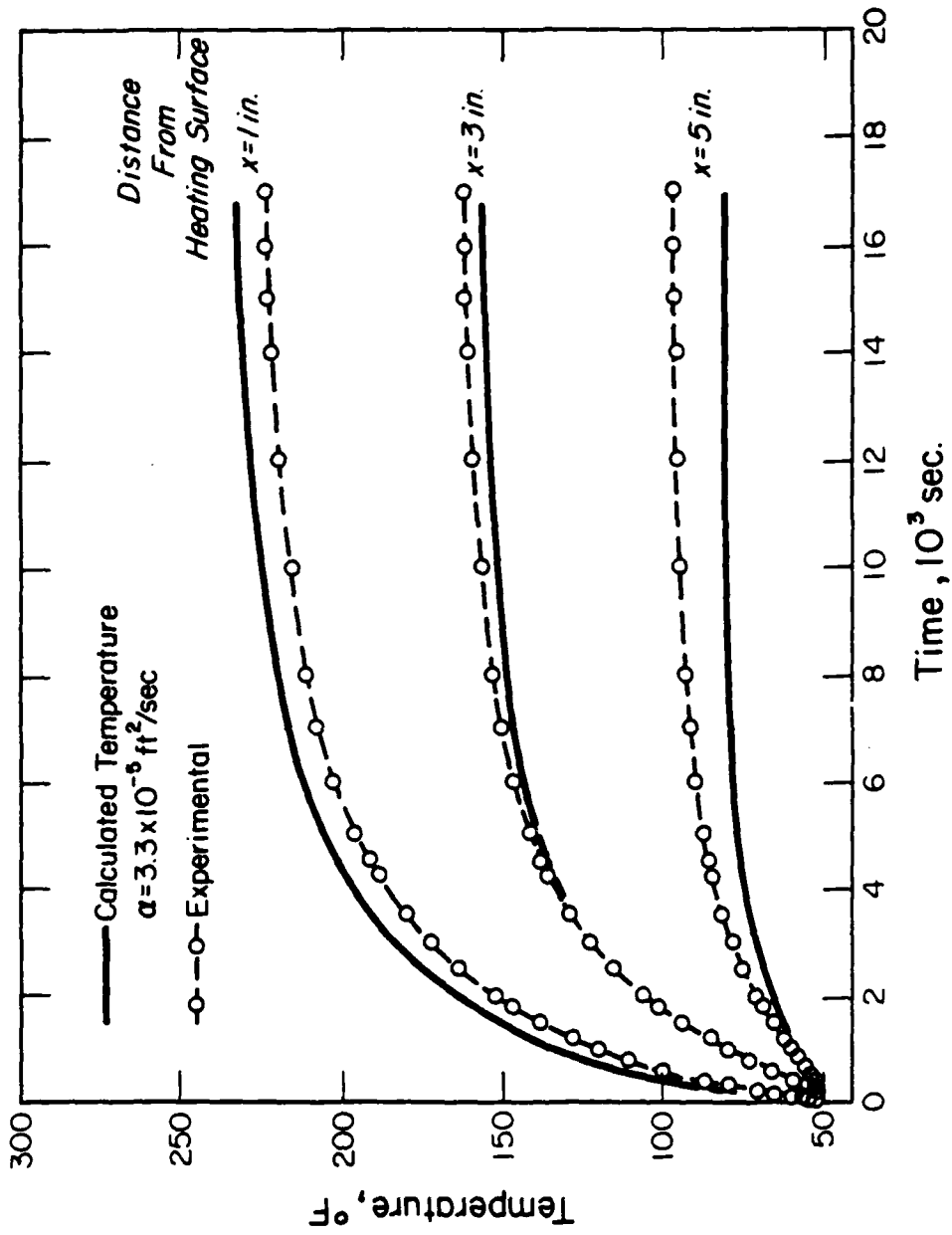


Figure 12. Comparisons of Calculated Temperature Responses Versus Experimental Values, Case XQ.

TABLE 1

## SUMMARY OF EFFECTIVE CONDUCTIVITIES AND EFFECTIVE DIFFUSIVITIES

Test Run	Effective Conductivity k (BTU/hr-°F-ft)	Effective Diffusivity $\alpha$ (ft <sup>2</sup> /sec)	Remarks
XQ	3.59	$3.3 \times 10^{-5}$	Heat flow along fiber axis. Configuration X, Figure 3.
XT	3.66	$3.0 \times 10^{-5}$	
Average	3.63	$3.15 \times 10^{-5}$	
YQ	0.452	$2.0 \times 10^{-6}$	Heat flow transverse to fibers and specimen slabs Configuration Y, Figure 3
	0.459	$2.7 \times 10^{-6}$	
YT	0.431	$2.2 \times 10^{-6}$	
	0.451	$2.8 \times 10^{-6}$	
Average	0.448	$2.4 \times 10^{-6}$	
ZQ	0.700	$3.19 \times 10^{-6}$	Heat flow transverse to fibers, parallel to slabs Configuration Z, Figure 3
ZT	0.590	$2.71 \times 10^{-6}$	
Average	0.645	$2.95 \times 10^{-6}$	
M	0.136	$8.5 \times 10^{-7}$	Heat flow normal to resin slabs, constant heat flux

extracted thermal diffusivity values are contained in Appendix A, which also includes the temperature-time records for test run XQ illustrated in this section.

Some comments are in order with regard to the effective thermal conductivities in the directions parallel and transverse to the fiber axis: the values reported are for an average temperature of 150°F and the

axial value is 8.10 times as large as the lower one of the two transverse values. In Reference [4], effective conductivities for 50 percent uni-directional fibrous composites are listed as 7.05 and 0.55 BTU/hr-°F-ft (at a temperature of 350°K) for the axial and transverse values, respectively. Their ratio is 13. A difference of the volume ratio 0.50 from the value used in this study may be partially responsible. However, the effective value of 7.05 reported in [4] is at considerable variance with the value of 3.63 given in Table 1; the difference may be attributed to the different tow structures and the different carbonization temperatures used in their respective processes.

## THERMO-PHYSICAL PROPERTIES OF THE CONSTITUENTS

Having obtained the directional values for the effective thermal conductivities and diffusivities, the next step was to deduce basic thermo-physical properties of the constituent materials. The scalar product ( $\rho C$ ) for the carbon/epoxy composite can be calculated from data obtained for each of the three configurations X, Y, and Z. Starting with the definition  $\rho C = k/\alpha$ , the effective thermal inertia values were obtained for each configuration; these values should conceptually agree, but have some variation as noted below:

From Configuration X:	$(\rho C) = 32.0 \text{ BTU/ft}^3\text{-}^\circ\text{F}$
Y:	$(\rho C) = 51.85 \text{ BTU/ft}^3\text{-}^\circ\text{F}$
Z:	<u><math>(\rho C) = 60.73 \text{ BTU/ft}^3\text{-}^\circ\text{F}</math></u>
Average	48.19

From Configuration M:  $(\rho C)_m = 44.4 \text{ BTU/ft}^3\text{-}^\circ\text{F}$   
(pure resin slabs)

It should be pointed out that the values for thermal inertia ( $\rho C$ ) for the composite specimens should agree with engineering accuracy based on the data from all three configurations X, Y, and Z. However, the data based on configuration X revealed some inherent inaccuracy in the reduction of the data to obtain the effective conductivity and effective diffusivity.

For this reason, less credence was placed on the  $(\rho C)$ -value from that configuration. It must also be recognized that the product term  $(\rho C)$  was obtained by dividing  $k$  by  $\alpha$ , both of which were deduced from the experimental data. In obtaining the ratio, errors in the individual numerical values were amplified. Taking the average of the three  $(\rho C)$ -values, an accepted result was:

$$(\rho C) = 48.2 \text{ BTU/ft}^3\text{-}^\circ\text{F, for composites.}$$

Further deductions for the basic thermo-physical properties of the constituents are discussed below.

1. DENSITY

Manufacturer's specifications for the prepreg that went into graphite/epoxy specimen gave the density values of 0.0660 and 0.0460  $\text{lb}_m/\text{in}^3$  for fiber and resin, respectively. Graphite-epoxy specimen slabs and resin slabs were weighed and their volumes noted in connection with the present study; from these observations, there resulted the following density values:

For composite (0.597 fiber, 0.403 resin by volume)

$$\rho = 0.0578 \text{ lb}_m/\text{in}^3$$

For resin

$$\rho_m = 0.0462 \text{ lb}_m/\text{in}^3 .$$

Since the density of a composite is related to the constituent densities by the relation:

$$\rho = \rho_f v_f + \rho_m v_m \quad (9)$$

its fiber density can be computed from Equation (9), with  $v_f = 0.597$ , and  $v_m = 0.403$ . This resulted in:

$$\rho_f = 0.0656 \text{ lb}_m/\text{in}^3 .$$

## 2. SPECIFIC HEAT

For the resin matrix, the values of  $(\rho C)_m$  and  $\rho_m$  gave the specific heat for resin as:

$$C_m = 0.556 \text{ BTU/lb}_m\text{-}^\circ\text{F} .$$

For fiber specific heat, the calculations were not as direct as for the resin matrix. First, the thermal inertia term  $(\rho C)$  for the composite was related to the inertia terms of the constituents by the relation:

$$(\rho C) = (\rho C)_f v_f + (\rho C)_m v_m . \quad (10)$$

The best values for  $(\rho C)$  of the composite and for  $(\rho C)_m$  of the resin matrix were inserted into Equation (10), with  $v_f$  and  $v_m$  at 0.597 and 0.403, respectively. The product  $(\rho C)_f$  for the fiber was determined to be:

$$(\rho C)_f = 50.8 \text{ BTU/ft}^3\text{-}^\circ\text{F} .$$



Since  $\rho_f$  has been determined as  $0.0656 \text{ lb/in}^3$ , the specific heat for carbon fibers was therefore:

$$C_f = 0.448 \text{ BTU/lb}_m - ^\circ\text{F} .$$

### 3. THERMAL CONDUCTIVITY

For the resin matrix, which was assumed isotropic, the thermal conductivity was listed in Table 1 as  $0.136 \text{ BTU}/(\text{hr-}^\circ\text{F-ft})$ .

For the fibers in the composite, there were three principal values. From the data obtained with heat flow parallel to the uni-directional fibers, the fiber conductivity along the fiber axis can be deduced based on a parallel heat flow circuit expressed by Equation (4). From Table 1, the effective conductivity for heat flow along the uni-directional fiber is given as  $3.63 \text{ BTU}/(\text{hr-}^\circ\text{F-ft})$ ; since  $k_m$  has been deduced, therefore the axial conductivity for fibers can be obtained.

$$k_{fa} = 5.99 \text{ BTU}/(\text{hr-}^\circ\text{F-ft})$$

along the fiber axial direction.

For the transverse conductivity across the fiber axis, the method of deduction was not as simple.

There were two measured values for the effective conductivities when heat flow is transverse to the uni-directional fibers. Normal to the slab-specimen plane, the effective value obtained was  $0.448 \text{ BTU}/\text{hr-}^\circ\text{F-ft}$ ; in the slab-specimen plane the effective value is  $0.645$ . Insofar as the dispersion pattern shown in Figure 1 exhibits no preferential

direction, the difference between these two values were the results of heat leakage to the side. In examining the experimental arrangements, the data obtained with heat flow normal to the slab-plane was considered more reliable since thermal grease was used to minimize the contact resistances at inter-slab locations among other factors considered.

In the analysis of [3], the hexagonal dispersion pattern was shown to produce equal effective conductivities regardless of the heat flow direction, therefore the question is now: what is the ratio of the fiber (transverse) conductivity to the matrix (isotropic) conductivity for a fiber-volume ratio of 0.597 such that the effective-to-matrix conductivity ratio is 3.29 ( $= 0.448/0.136$ )? By using a built-in subroutine (STAG), the ratio turned out to be 17.8 or the transverse conductivity of the fibers is  $17.8 \times .136 = 2.42$  BTU/hr- $^{\circ}$ F-ft<sup>2</sup>/ft. Hence, the fibers were shown in the above analysis to have two conductivities as follows:

- (i) Along the fiber axis:  $K_{fa} = 5.99$  BTU/hr- $^{\circ}$ F-ft<sup>2</sup>/ft
- (ii) Transverse to the fiber axis:  $K_{ft} = 2.42$  BTU/hr- $^{\circ}$ F-ft<sup>2</sup>/ft

There were very few data reported in the literature; the only publication which listed the axial conductivity for carbon fibers was that of Larsen [5], who reported a value of 2.5 BTU/hr- $^{\circ}$ F-ft<sup>2</sup>/ft which was about one-third of the value measured in this study. It is of interest to note that the isotropic conductivity of resin matrix was also given by Larsen in Reference [5], as 0.133 BTU/hr- $^{\circ}$ F-ft<sup>2</sup>/ft which was in excellent agreement with the value of 0.136 measured in this experimental work.

Another value for the axial conductivity of carbon fibers was deduced from the data found in Reference [4]. An axial effective conductivity for a 50 percent carbon-epoxy composite (uni-directional) was listed as  $0.117 \text{ W/C}_m\text{-}^\circ\text{K}$ , or  $6.76 \text{ BTU}/(\text{hr-}^\circ\text{F-ft})$  for a temperature of  $150^\circ\text{F}$ . Using Equation (4) to synthesize for the fiber axial conductivity, a value of  $k_{fa} = 13.4 \text{ BTU}/(\text{hr-}^\circ\text{F-ft})$  was obtained. (In doing so,  $k_m$  was set at 0.136, which, even if inaccurate, hardly affected the result.) From these sources, then, the axial conductivity for carbon fibers ranged from  $2.5 \text{ BTU}/(\text{hr-}^\circ\text{F-ft})$  found in Reference [5] to  $13.4 \text{ BTU}/(\text{hr-}^\circ\text{F-ft})$  based on the data of Reference [4], while the value determined in this investigation turned out to be  $6.0 \text{ BTU}/(\text{hr-}^\circ\text{F-ft})$ . The variation was considerable indeed.

## VI

### CONCLUSIONS

The purposes of this experimental investigation were twofold: one was to explore the thermal physical properties of a carbon/epoxy composite, a frequently used material in aerospace structures, and the other was to develop a reliable measurement method to determine these properties by using carbon/epoxy materials as an example. By employing a transient heat flow technique, the effective thermal conductivities and diffusivities along three principal directions were determined for carbon/epoxy composites with uni-directional fibers; uni-directional orientation was chosen because it afforded a simpler geometry of the dispersion pattern of the fibers than other dispersion prescriptions.

The thermal conductivities of the constituents - the fibers and the matrix - of the composites were determined by first establishing the dispersion pattern of the fibers through microscopic photographic examinations of the specimen cross-section, illustrated in Figure 1; and by using the relation between the effective-to-matrix conductivity ratio and the fiber-to-matrix conductivity ratio obtained in Reference [1] or AFWAL-TR-80-3012.

With regard to the micro-structure of the carbon/epoxy composites prepared from plies, microscopic examinations indicated, generally speaking, a uniform dispersion pattern very much resembling a staggered

arrangement into hexagonal arrays. An unusual feature was the excess matrix (resin) materials which congregated near the interfaces between plies and formed a canal-like border of one-tenth the thickness of an entire ply. Thus, in the cross section plane, the structural pattern was not homogeneous macroscopically and this factor contributed to the difference between the two transverse effective thermal conductivities, and led undoubtedly to different elastic properties in these two transverse directions as well. Further investigations are needed to clarify the observed discrepancy.

The method of synthesizing the transverse effective thermal conductivities to obtain fiber-to-matrix conductivity ratios was based on an exact mathematical analysis [3]; in the range of this experimental investigation--fiber/epoxy composites with 0.60 fiber content by volume--the relationship was such that a large change in the fiber/epoxy thermal conductivity ratio produced a relatively small change in the effective conductivity ratio. Since the inverse process was used for synthesis, i.e., from an effective value to the constituent value, the process was therefore somewhat insensitive, and for further work, composites with low volume ratios for fibers are more desirable from the sensitivity standpoint.

The measurements conducted in this study were limited by instrumentation problems to a level of 250°F. Since fiber/epoxy composites are known to exhibit temperature-dependence of their thermal properties, future efforts are required to extend the temperatures to a more practical range.

APPENDIX A

TEMPERATURE DATA AND COMPARISONS WITH PREDICTIONS

In the following pages, the temperature-time records are presented for the test runs on composite specimens in configurations X, Y, and Z as well as on matrix (resin only) specimens. For clarification of these configurations, reference is made to Figure 3, page 15. Two tests were performed for each configuration, one with the heating surface at a constant heat flux condition and the other, at a constant surface temperature condition.

Experimental data shown in dashed lines are compared with theoretical predicted values which are based on the diffusivity values obtained by a best fit of the experimental curve with the theoretical prediction for the central point, midway between the heating and cooling surface. These two measured surface temperatures were used as the boundary conditions in obtaining the interior temperature-time histories. The best-fit thermal diffusivity values for each test run are listed in Table 1, page 34.

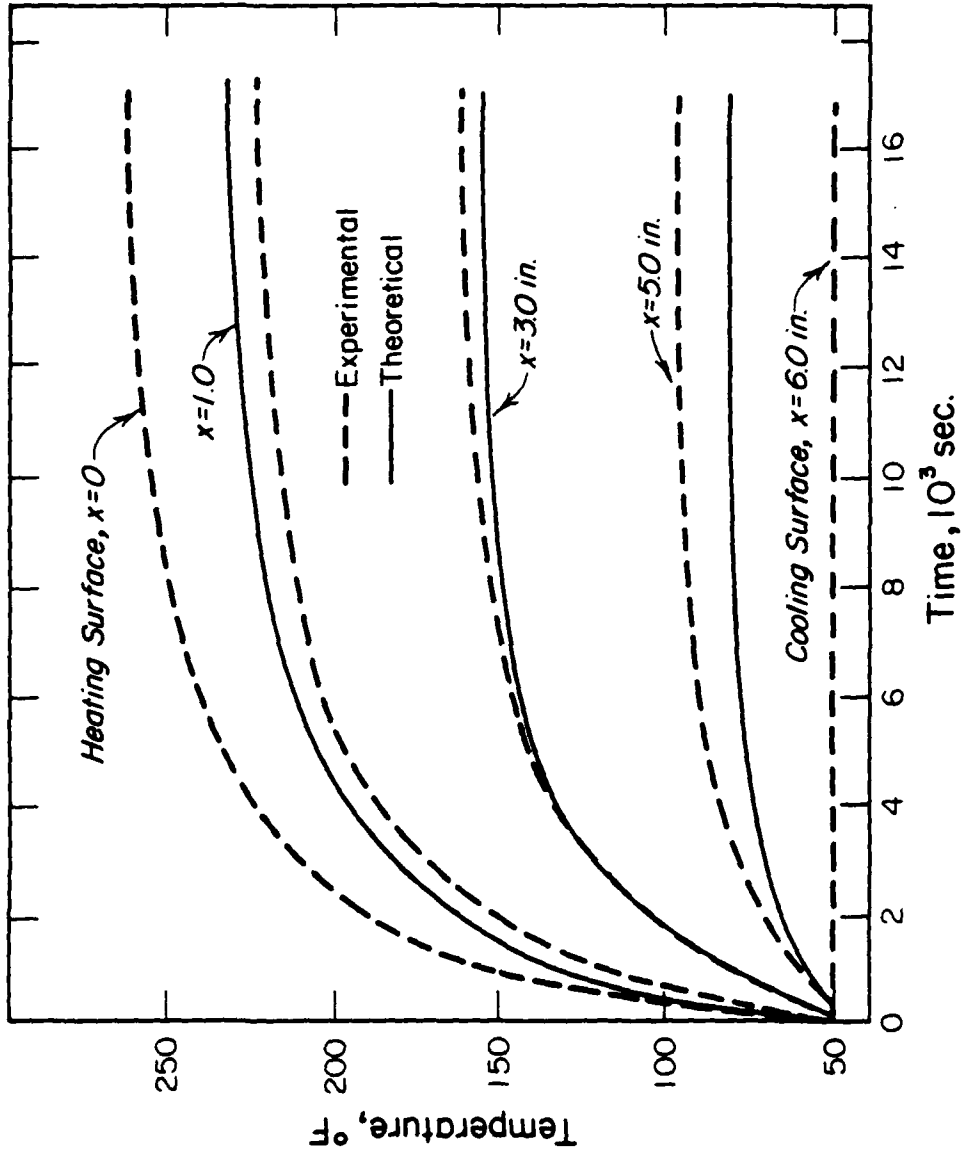


Figure A-1. Temperature Profile Matching Results, Configuration X, Constant Heat Flux ( $XQ$ ).



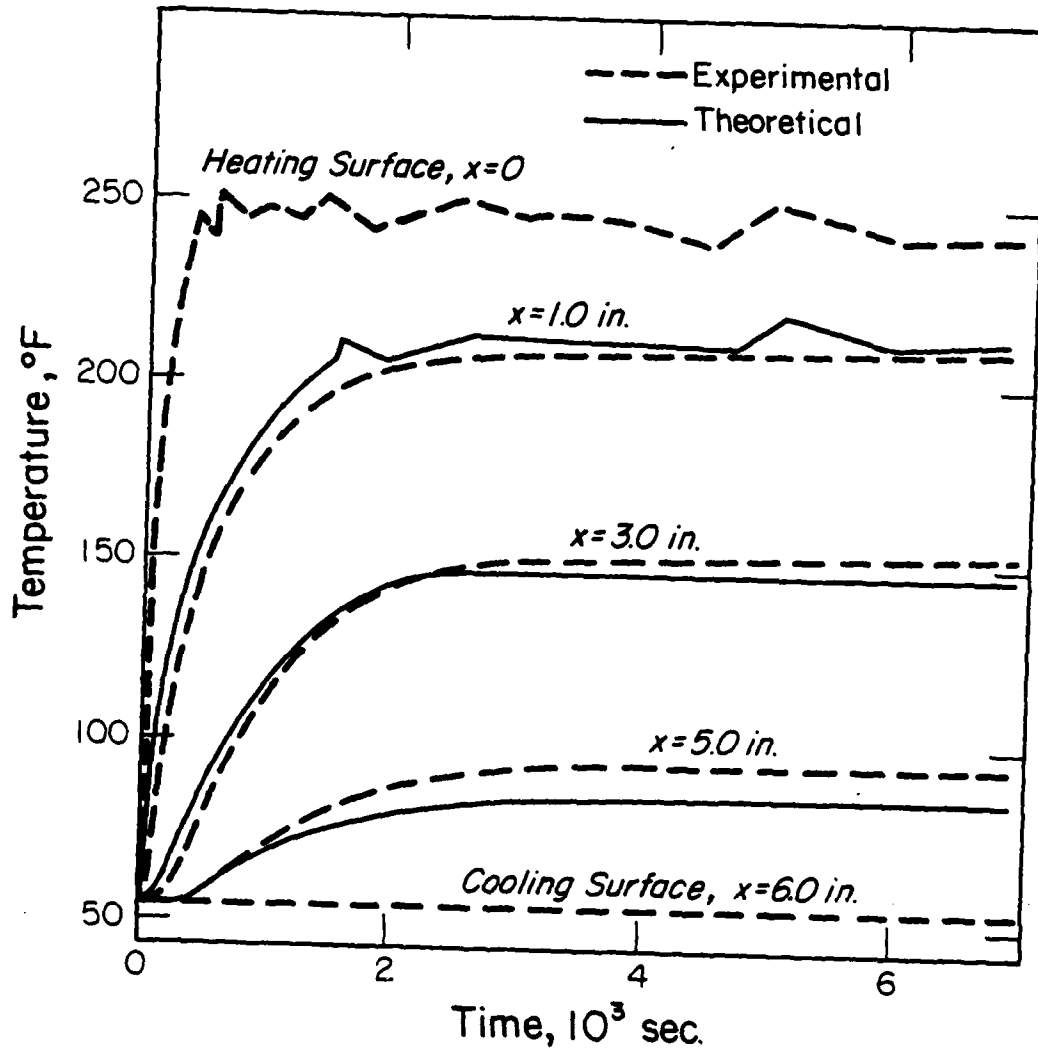


Figure A-2. Temperature Profile Matching Results, Configuration X, Constant Surface Temperature (XT).

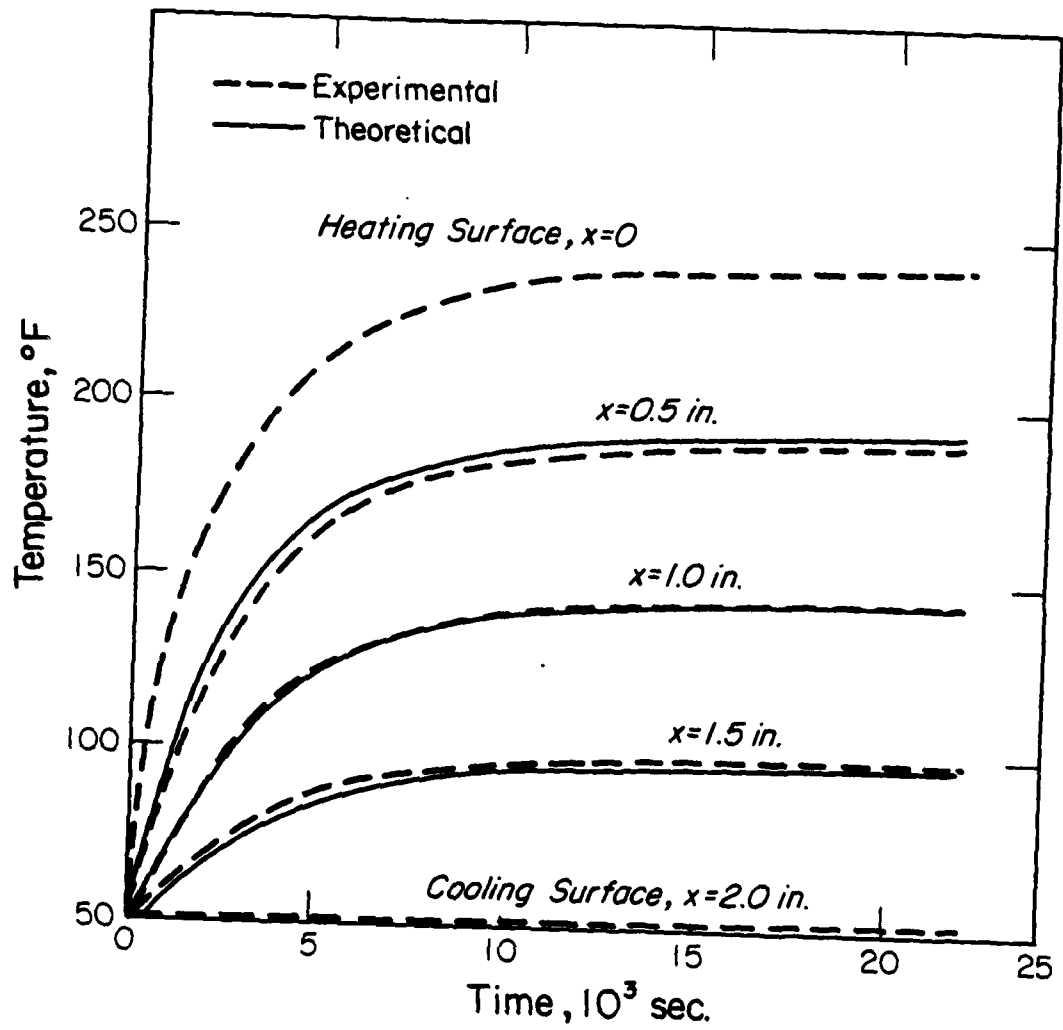


Figure A-3. Temperature Profile Matching Results, Configuration Y, Constant Heat Flux (YQ1).

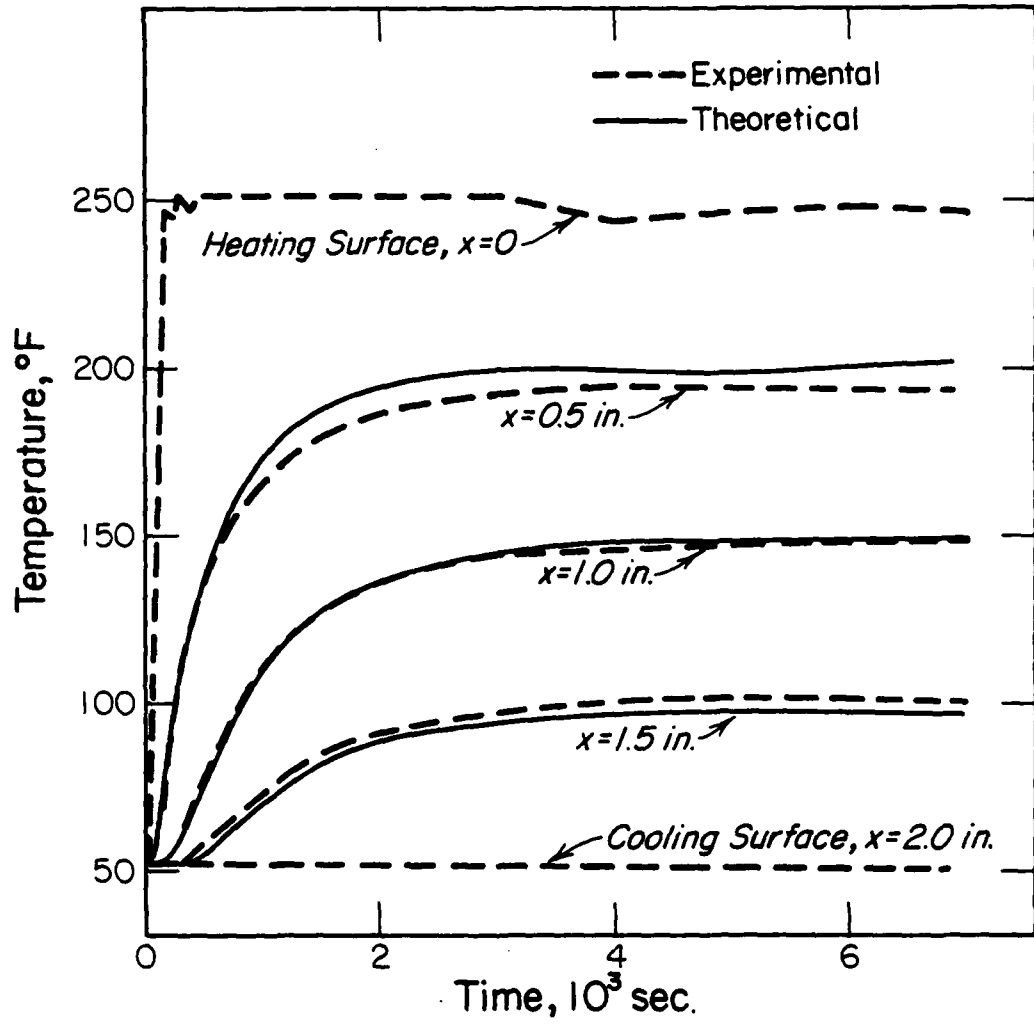


Figure A-4. Temperature Profile Matching Results, Configuration Y, Constant Surface Temperature (YT1).

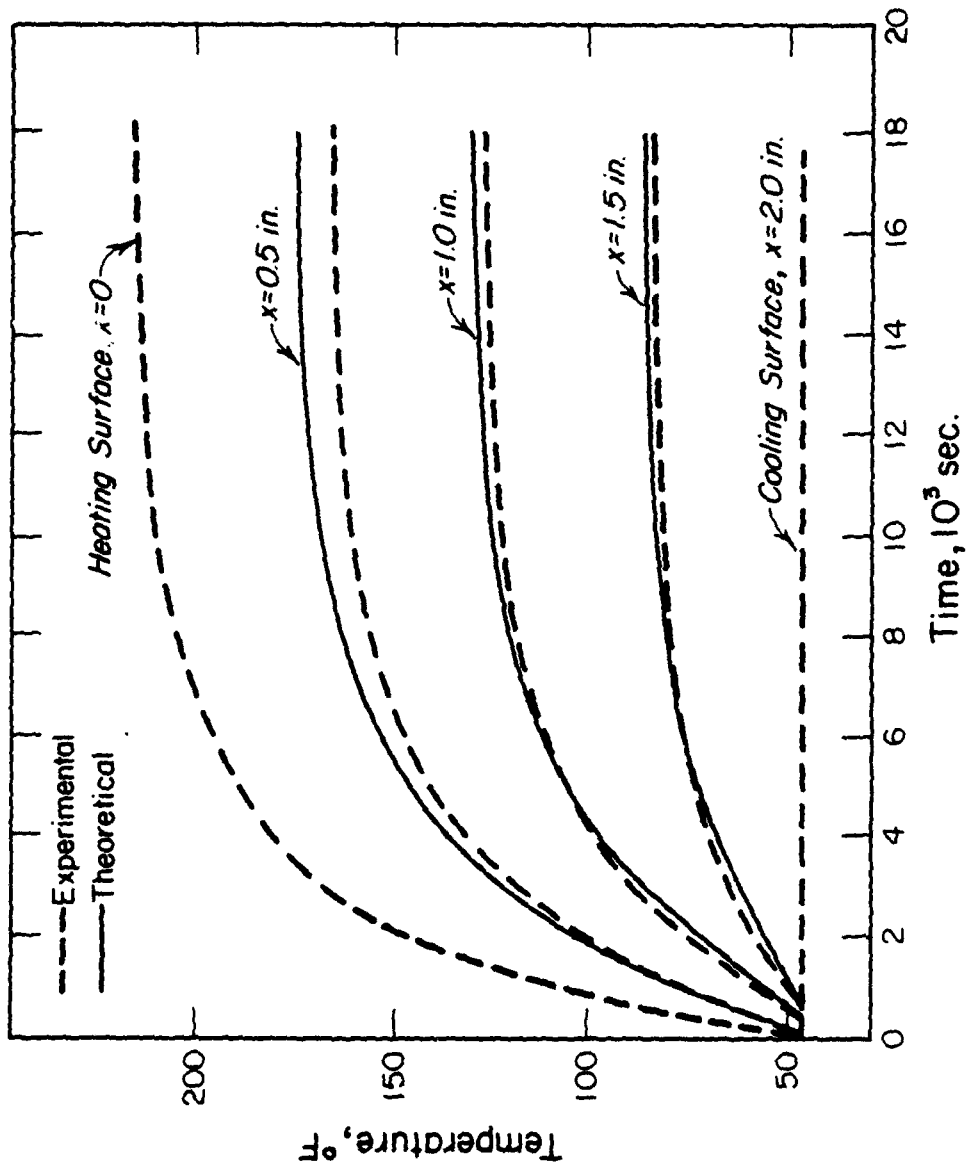


Figure A-5. Temperature Profile Matching Results, Configuration Y, Constant Heat Flux (YQ2).

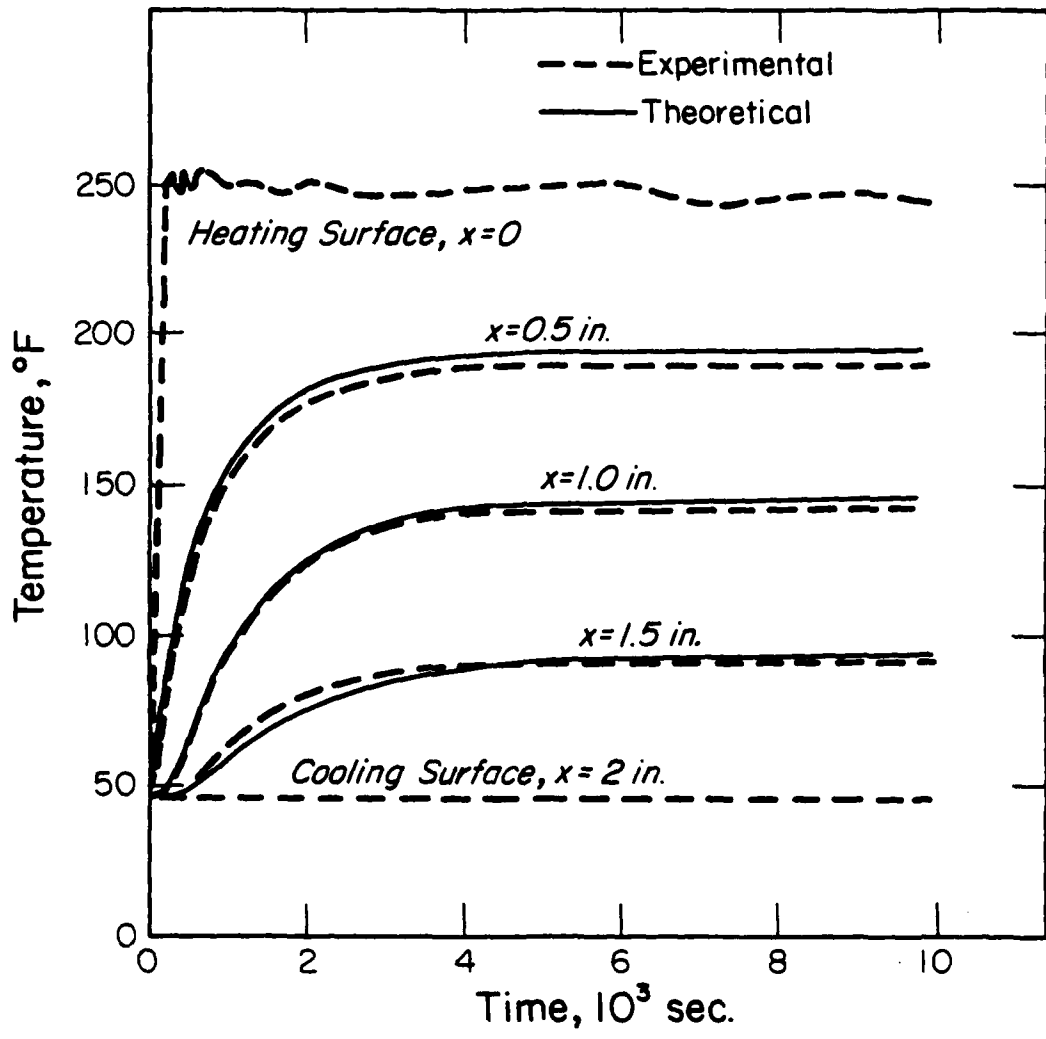


Figure A-6. Temperature Profile Matching Results, Configuration Y, Constant Surface Temperature (YT2).

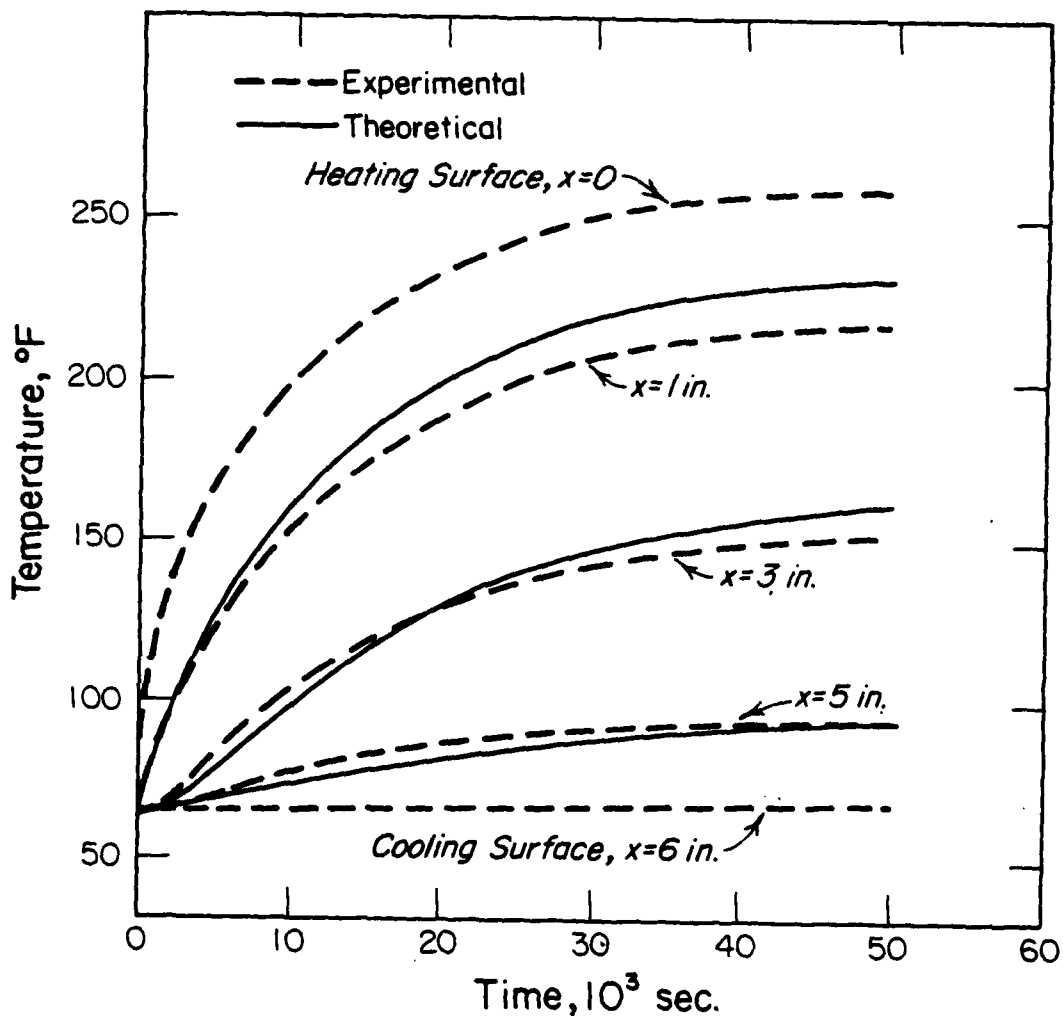


Figure A-7. Temperature Profile Matching Results, Configuration Z, Constant Heat Flux (ZQ).

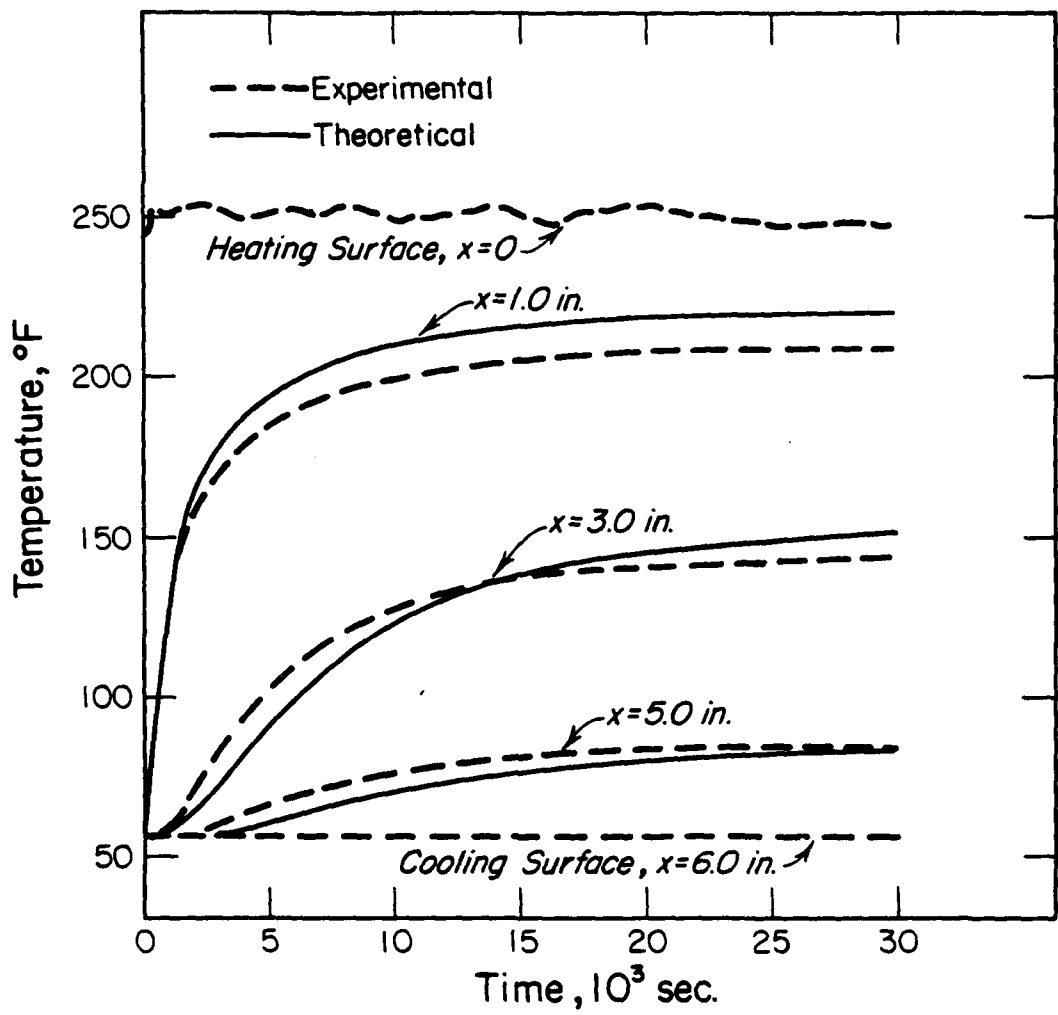


Figure A-8. Temperature Profile Matching Results, Configuration Z, Constant Surface Temperature (ZT).

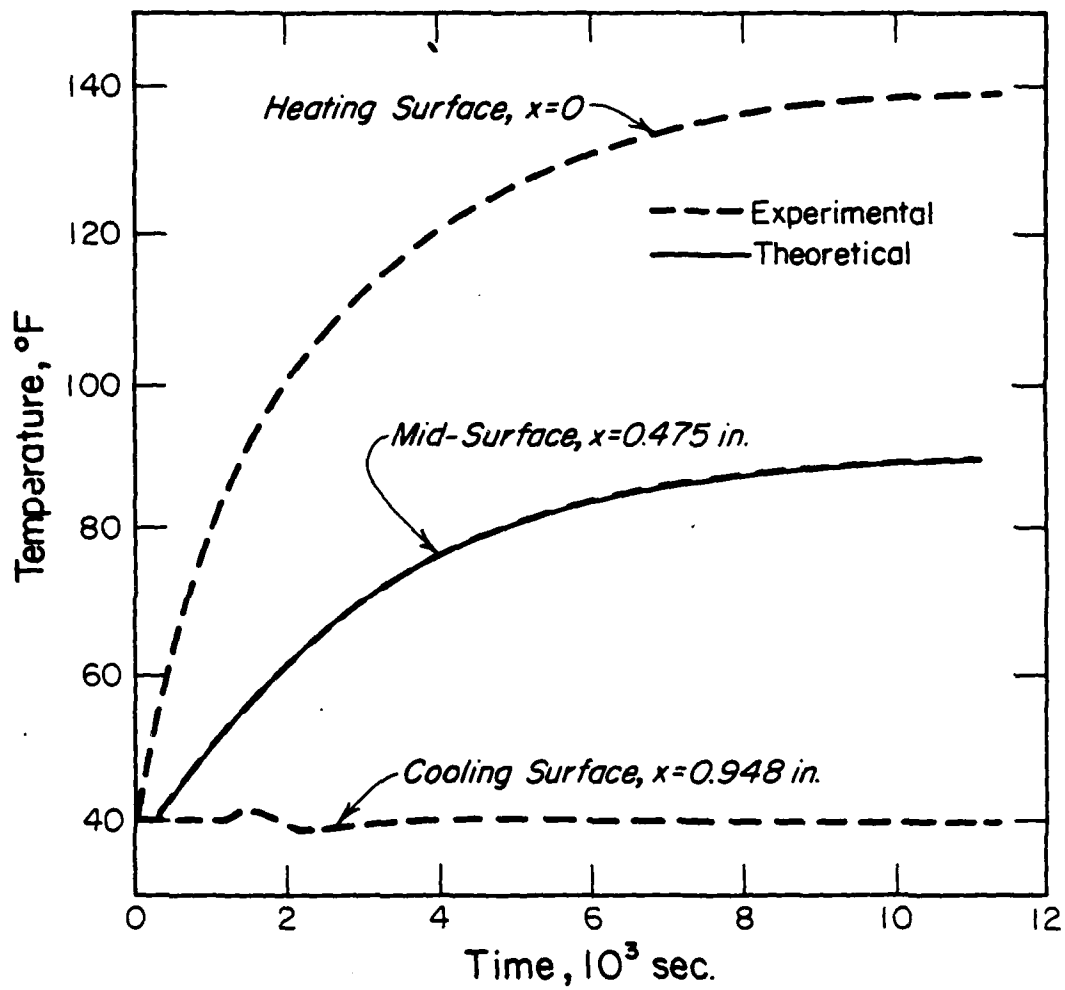


Figure A-9. Temperature Profile Matching Results, Resin Specimen, Constant Heat Flux (M).



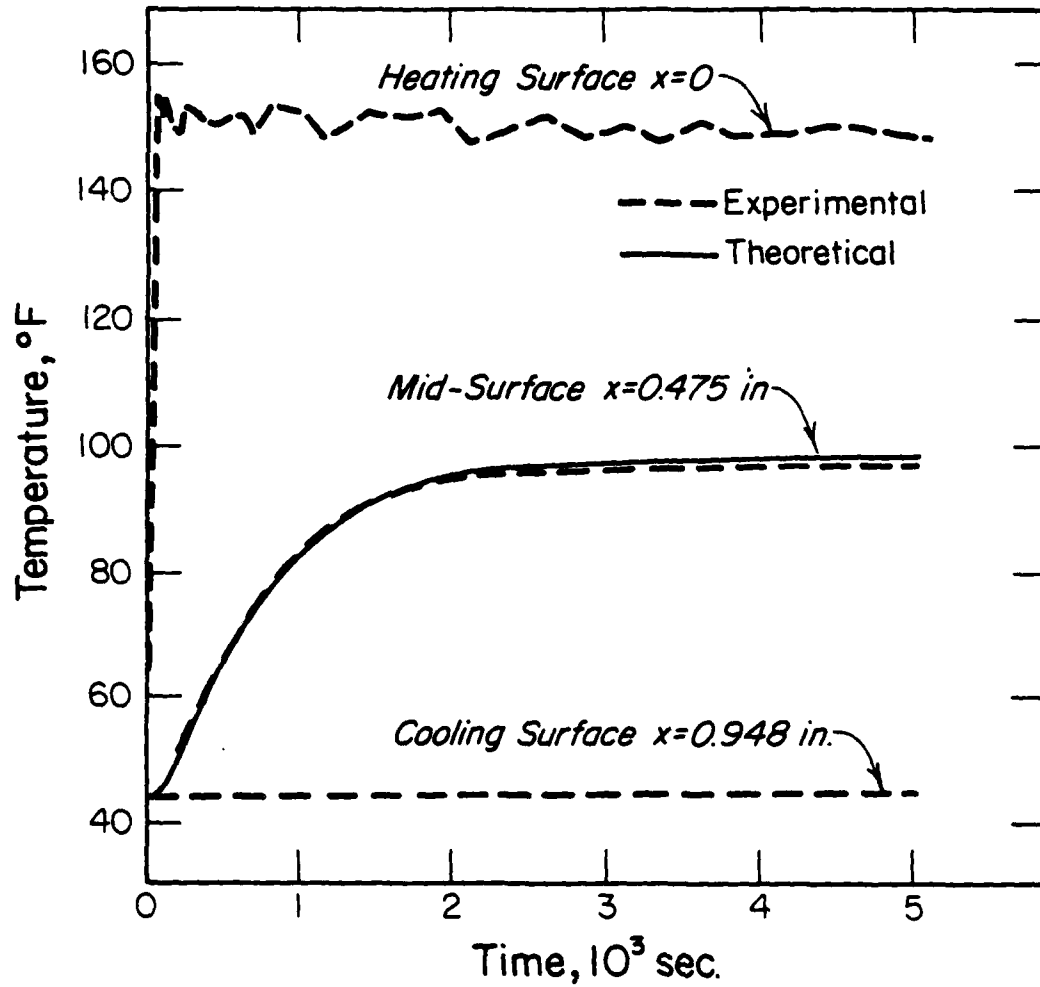


Figure A-10. Temperature Profile Matching Results, Resin Specimen, Constant Surface Temperature (MT).

APPENDIX B  
VOLUME-RATIO STUDY

The volume ratio of the graphite-epoxy composite used in this study was calculated by visually counting and measuring the fibers (in reality, tows of fibers) in a given cross-sectional area, similar to Figure 1. An enlarged photograph of the composite, 250X, was sectioned into fifteen equal units of approximately two-hundred fibers each, and the average number of fibers per unit was determined. Then one section was enlarged, overall magnification 2100X, and one-hundred fiber diameters, randomly chosen, were measured. The diameter measurement was repeated in order to assuage individual observational bias. Next, the diameters (actually the squares of the diameters) were given a statistical distribution test, the  $\chi$ -square test, which showed that the quantity  $D^2$  did follow a normal (Gaussian) distribution. An average image diameter,  $\bar{D} = 0.630$  inches, was obtained from the second enlargement (which corresponded to an actual average diameter of 0.0030 inches\*), and was therefore assumed to apply to the other fourteen counting units.

$$V = \bar{N}_f (\pi \bar{D}^2 / 4A)$$

---

\*Hercule's specifications say that the ply thickness is 0.005 inches, so the value for the fiber diameter is compatible.

v = volume ratio

$\bar{N}_f$  = average number of fibers in the area counted

$\bar{D}^2$  = square of the average diameter

A = counting area

The entire process gave a fiber volume ratio of 59.7 percent with a 4 percent standard deviation, i.e., the volume ratio lies within the limits of 55.7 to 63.7 percent with 59.7 as the most probable range. The population distribution for the quantity  $D^2$  (D = image diameter, inches) for the first counting unit is shown in Figure B-1.

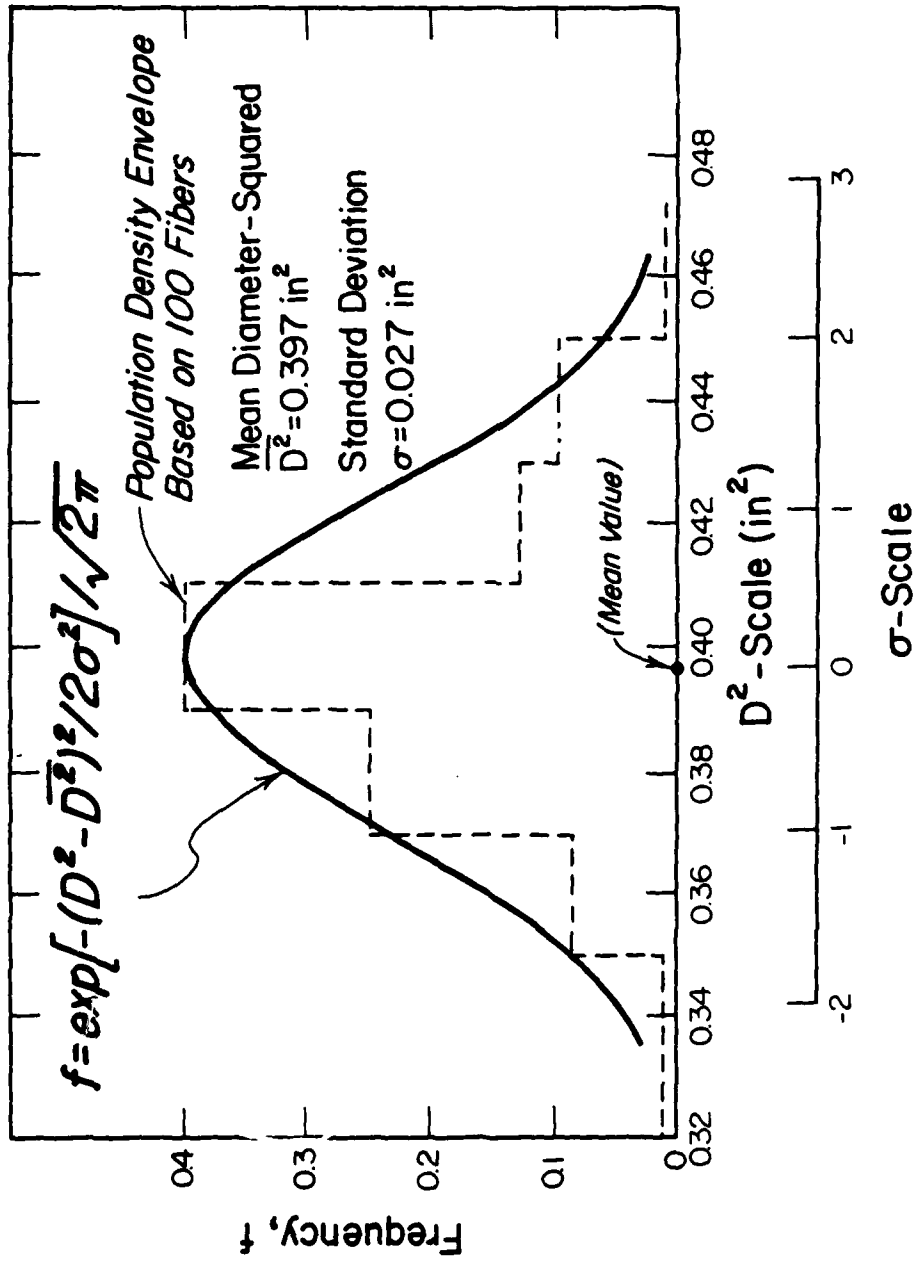


Figure B-1. Fiber Diameter Population Distribution.

APPENDIX C  
EQUIPMENT DESCRIPTION

The purpose of the experimental apparatus was to generate and record transient temperature data present in the graphite-epoxy block. In order to accomplish this, equipment was obtained which controlled the temperature at the heating face and cooling face, monitored and recorded transient temperature data, and insulated the graphite-epoxy test specimen.

Enclosed herein is the following: a summary of the equipment which was used to conduct the two experiments, a detailed description of equipment items and experimental procedure; a section outlining the function of the three equipment groups, i.e., temperature control system, the insulation, temperature measurement system, and finally a specification list of the individual equipment.

Two boundary conditions were imposed at the heating face of the graphite-epoxy composite: one was a constant heat flux,  $Q$ , and the other was a constant temperature step,  $T$ . Table C-1 summarizes equipment used in each experiment. The two experiments were then conducted as follows:

#### Constant Surface Temperature Experiment (T)

Equipment items used for this part of the experiment and their interconnections are illustrated in Figure C-1. Temperature signals from

TABLE C-1  
SUMMARY OF EXPERIMENTAL EQUIPMENT

Equipment	Experiment	Case
Variable Transformer	Q	All
Temperature Controller	T	All
Clock	T	All
Digital Voltmeter	Q,T	All
Watt Transducer	Q,T	All
6" x 6" Heating Plate	Q,T	Y
3" x 6" Heating Plate	Q,T	X,Z
Thermal Feedback Sensor	T	All

the test cell were recorded by a Fluke Data Logger, and simultaneously, the cooling plate temperature was monitored by a thermocouple reader. For maintaining the surface temperature at a pre-set value, a temperature controller (Chromalox 3804) was used to sense the surface temperature of the specimen block and adjust the power-supplier accordingly. A timing device, built into the circuit, monitored the duration in which power was supplied to the heater; in this way the integrated power input could be obtained, which was later needed for steady-state calculations of the thermal conductivity values. The power supply rating was displayed through a Watt transducer (PT 2501F, Bell). The assembled items are pictorially presented in Figure C-2; this also shows the cooling tank for



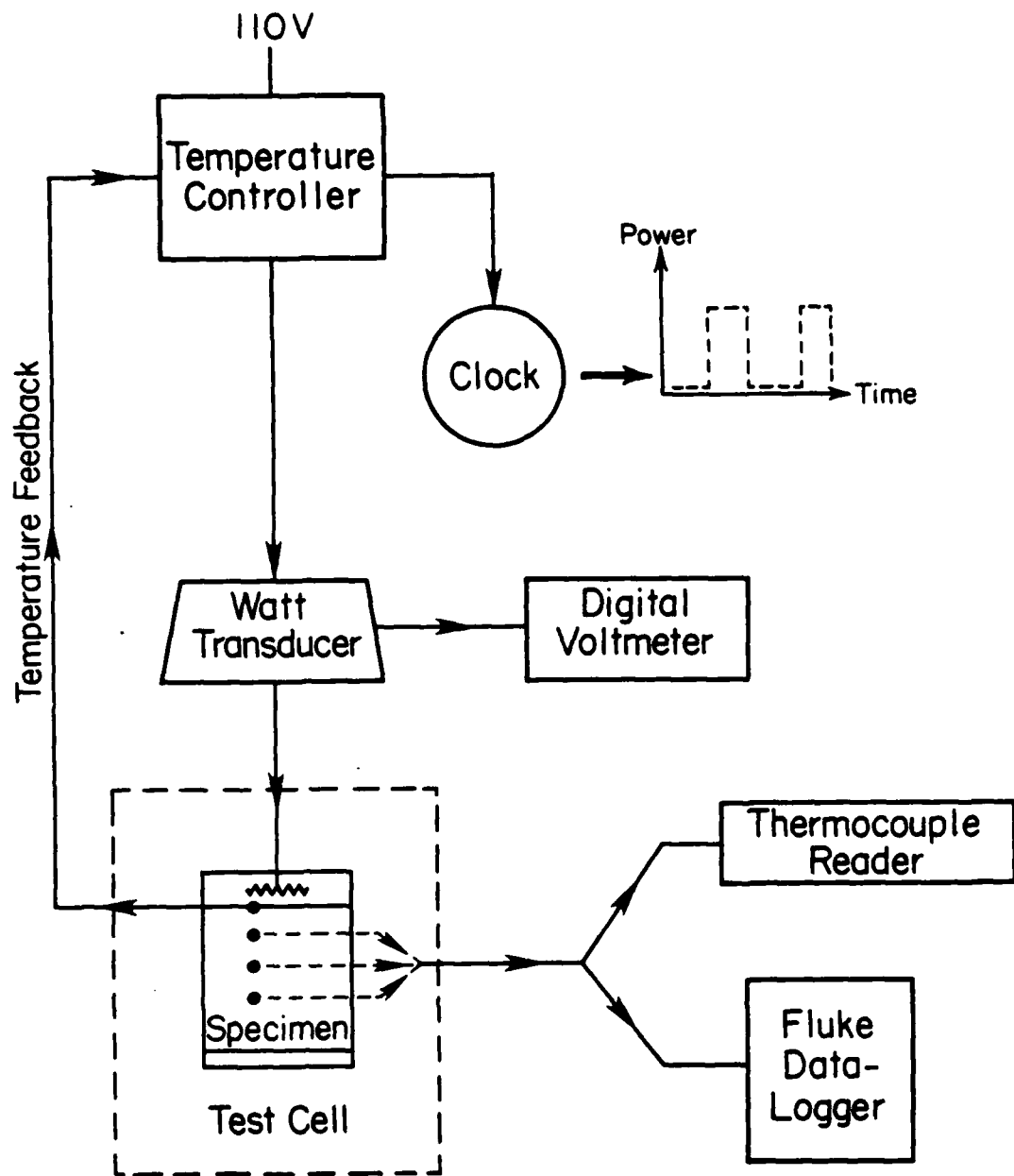


Figure C-1. Schematic of Experimental Arrangement for Constant Surface Temperature Test.



Figure C-2. Assembly of Experimental Equipment.

maintaining the cooling surface temperature.

The sequential steps in conducting this experiment consisted of the following:

1. The test block was placed inside the test chamber, as illustrated in Figure 4, and all electrical leads were connected to their proper terminals.
2. The cooling tank valve was opened to cool the specimen to its initial temperature, approximately 50°F. This temperature was assumed to have been reached after the temperature gradient in the test cell was less than or equal to 0.5°F.
3. The temperature control was then set so that the temperature at the heating face was equal to the initial temperature of the test cell plus 200°F. Upon reaching its initial condition, a constant step change in temperature was imposed via the temperature controller.
4. Temperatures inside the test cell were recorded at the heating face, and at three locations between the two boundary plates.
5. The temperature at the cooling plate was monitored continuously and kept within 0.5°F limit. The heating plate was controlled by the temperature controller; its temperature oscillated no more than 5°F as a consequence.
6. Data were recorded at approximately 5 to 10°F intervals by the Data Logger such that a smooth temperature profile could be constructed.
7. Steady state and the conclusion of the experiment were assumed after the temperature change at all stations was less than 0.2°F/1000 seconds.

8. At the conclusion of the experiment, the following information was recorded:

- (i) initial conditions
- (ii) temperature profile at steady state
- (iii) average wattage supplied,  $Q$
- (iv) operational time, "on-time" of the Chromolox temperature controller,  $t_c$
- (v) total elapsed time of the experiment  $t_o$
- (vi) fiber orientation
- (vii) power required at steady state,  $q = Q(t_c/t_o)$

#### Constant Flux Experiment (Q)

The equipment items used in this experiment were essentially similar to those employed in the constant surface temperature part. The chief difference was that a variable transformer was used in the constant heat-flux experiment in lieu of the PID-controller, and also, the timing device was disconnected. The apparatus schematic is illustrated in Figure C-3. Temperature signals from the test cell were recorded by the Fluke Data Logger, and the cooling plate temperature was monitored simultaneously by a thermocouple reader. Finally, the amount of power supplied to the heating plate was also monitored using a Watt transducer.

In order to effect a  $200^{\circ}\text{F}$  temperature gradient between the heating and cooling plate, the power setting on the variable transformer had to be known. This value of power setting was obtained from the constant surface-temperature experiment. The experiment was then conducted as follows:

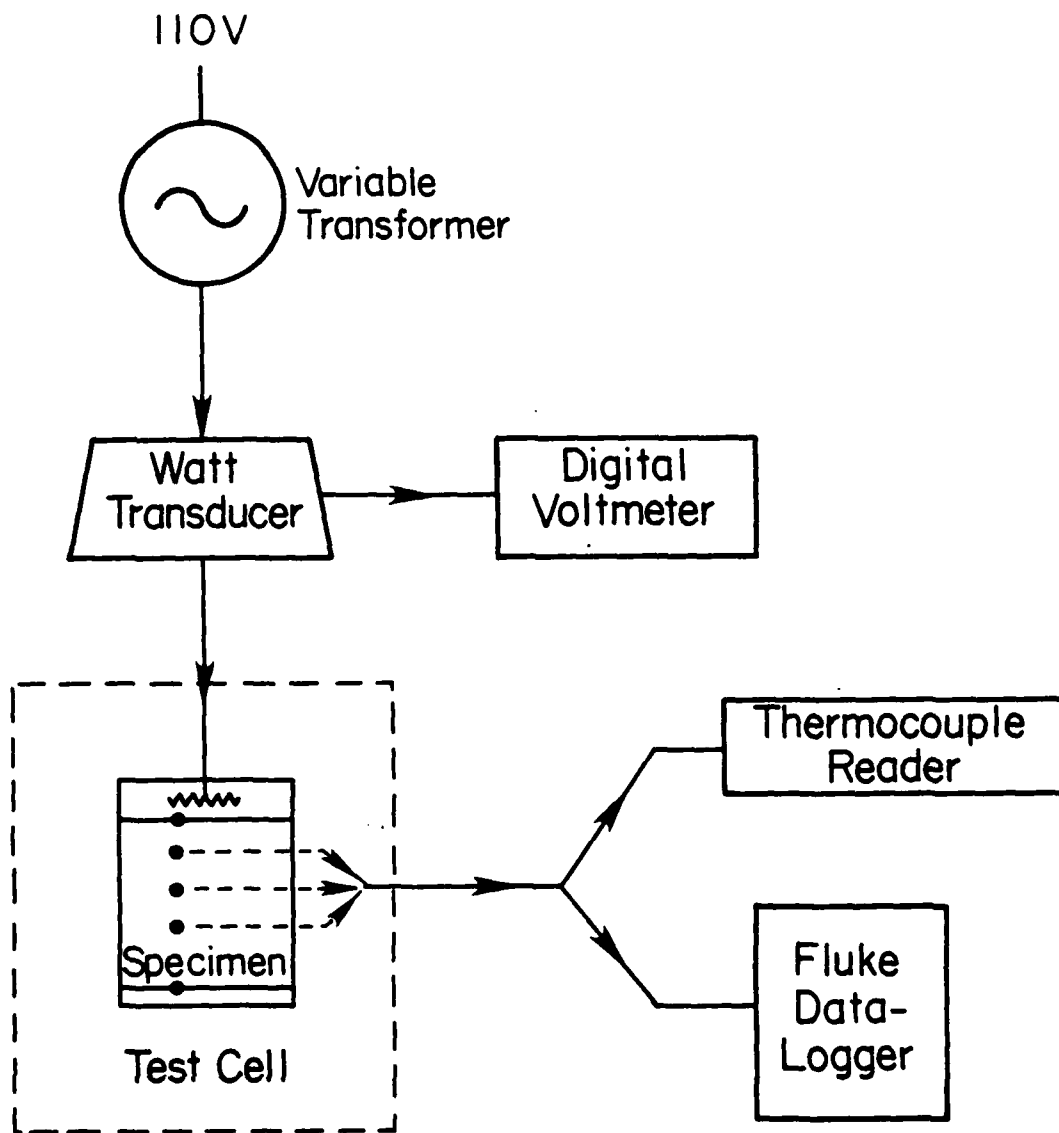


Figure C-3. Schematic of Experimental Arrangement for Constant Heat Flux Test.

1. The test block was assembled into the test cell, and connected to the proper equipment.
2. The cooling tank valve was opened to cool the specimen to its initial temperature, approximately 50°F; this took from five to ten hours. A uniform, initial temperature was assumed when the temperature variation in the test cell was less than or equal to 0.5°F.
3. The variable transformer was then set so that a temperature gradient of 200°F would result across the graphite-epoxy block at the conclusion of the experiment.
4. The temperatures inside the test cell were recorded at the heating face, cooling face, and three locations inside the graphite-epoxy test block.
5. The temperature at the cooling plate was monitored continuously and kept within 0.5°F. The heating plate was controlled by the variable transformer.
6. Data were recorded at approximately 5 to 10°F intervals by the Data Logger such that a smooth temperature profile could be constructed.
7. Steady state and the conclusion of the experiment was assumed when the temperature rise at all stations was less than 0.2°F/1000 seconds.
8. At the conclusion of the experiment, the following information was recorded:
  - (i) initial condition
  - (ii) temperature profile at steady state
  - (iii) average wattage supplied

- (iv) total elapse time of the experiment
- (v) fiber orientation

### Temperature Control System

#### (i) Heating System

The object of the heating system was to impose a boundary condition at the heating plane surface. It consisted of a power supply and an electrically resistant heating plate. Two different power supply units were used in the experiments: one was a variable transformer and the other, a proportional-integral-differential (PID) temperature controller. The transformer was used in those experiments requiring a constant heat flux,  $Q$ ; and the PID-controller was used in the alternate experiments for a temperature step change,  $T$ .

Two heating plates, a 3 x 6 x 0.0625 inch and a 6 x 6 x 0.0625 inch, were built. The rectangular heating plate, 3 x 6, was constructed by sandwiching three 1 x 6 inch heating strips between two 3 x 6 inch aluminum plates. The strip heaters were then wired in parallel, and the heating plate was instrumented with three iron-constantan thermocouples--one per heating strip. The center thermocouple was used to monitor the temperature of the heating plate surface, and the outside thermocouples were connected in parallel and used either as a feedback signal to the PID-controller or as a check of the center, recorded temperature. The 3 x 6 heating plate was used with the graphite-epoxy composite configurations X and Z.

The 6 x 6 heating plate was built in the same manner as the 3 x 6 plate. A 6 x 6 electrically resistant heating strip was placed between

two 6 x 6 inch aluminum plates and instrumented with three iron-constantan thermocouples. Two thermocouples were wired in parallel and were used to record the temperatures of the heating plate surface. The third thermocouple was used either as a signal feedback to the PID-controller or as an extra recorded temperature data point. The 6 x 6 heating plate was used during those experiments for configuration Y.

(ii) Cooling System

The purpose of the cooling system was to reduce the temperature of the graphite-epoxy test specimens to an initial temperature and to maintain the boundary condition at the cooling plane. The cooling system consisted of the following items:

- 1) cooling tank, 30 gallons
- 2) cooling plates, 6 x 6 x 1 inch
- 3) catch tank, 10 gallons
- 4) return pump, 20 gallons per minute
- 5) thermocouple indicator, iron-constantan

Water was cooled with ice in the cooling tank to approximately 50°F and then circulated through the cooling plates into the catch tank and back to the cooling tank. Constant temperature at the cooling plate was maintained by operator observation. Three thermocouples were attached to the cooling plates; two were wired in parallel and connected to the Data Logger, and the third was attached to the thermocouple indicator and monitored continuously. A change in temperature plate of more than 0.5°F was corrected by the operator manually.



### Insulation

The insulation provided an adiabatic condition on the peripheral surfaces of the graphite-epoxy specimens, and this shell, or test cell, was then placed into a fiberglass-insulation chamber. The insulation chamber was built using approximately fifty, 4' x 4' x 2" fiberglass panels. The chamber itself was approximately 4-foot cube, and the test cell was placed into the center of the cube. The R-value of the insulation at the center was approximately equal to 90, i.e.,  $k = 1.12 \times 10^{-2}$  BTU/(ft-hr-°F).

### Temperature Recording System

For recording the boundary temperatures and the transient temperatures inside the graphite-epoxy composite, the system consisted of a Fluke Data Logger and multi-junction, iron-constantan thermocouples. Three thermocouples were wired in parallel, thus forming a single group of parallel-junction thermocouples. Three groups of these were made. The three parallel-junction thermocouples were then attached to one of the graphite-epoxy specimens. In the graphite-epoxy composite, shallow grooves, approximately 1/8 x 1/8 inch were milled at 1, 3, and 5 inches from the heating face, and the three parallel-junction thermocouples were cemented below the plane surface near the geometrical center. Two such plates were built, and this procedure was used for configurations X and Z. Temperatures were recorded at the heating face, the cooling face, and the three inside stations.

For configuration Y, three thermocouples were wired in parallel forming a multi-junction thermocouple, and then attached to an aluminum

plate. The aluminum plate was 6 x 6 x .03 inches with three parallel slots cut through it. One slot was 3 inches long, and bisected the 6 x 6 aluminum plate. The other two slots were offset 0.5 inches on either side of this first slot. The thermocouples lead wires were placed in these slots, below the surface of the plate. Three such plates were made and placed at 0.5, 1.0, and 1.5 inches from the heating plate. The temperatures were then recorded at these three locations and at the heating and cooling face.

#### Graphite-Epoxy Composite

The graphite-epoxy composite samples were obtained from: Flight Dynamics Laboratory (Mr. Robert Achard), Wright-Patterson Air Force Base, Ohio.

The material used in the composites was manufactured by Hercules Incorporated, Utah. The physical properties of the composite as supplied are listed below (per specification).

Materials:     graphite fiber, epoxy matrix; 3501-5A, AS-1  
                  12 inch prepreg tape  
                  40 to 42 percent resin content  
                  fiber density (lb/in<sup>3</sup>) 0.0660  
                  resin density (lb/in<sup>3</sup>) 0.0460

#### Composite Properties:

                  packing arrangement,     random\*

---

\*Data were determined in this investigation. All other values on this page were provided by the manufacturer.

	volume ratio,	60 ± 4 percent*
		62 ± 3 percent
	fiber orientation	0 degrees
	density (lb/in <sup>3</sup> )	0.5785*
	(g/cm <sup>3</sup> )	1.604*
	void content, volume %	0
Geometry:	length (in)	6.0
	width (in)	6.0
	thickness (in)	0.5
	construction	105 lamina

Temperature Controller

Manufacturer	Chromalox, Lavergne, Tennessee
Model	3804 PID
Type	J, Iron-constantan
Range	0 to 400°F
Supply	120 VAC, 50/60 Hz.

Data Logger

Manufacturer	John Fluke Mfg. Co., Mountlake Terrace, WA.
Model	2240A
Type	J, K, T, or R
Scanners	10 channels/second
Scan speed	2.5 channels/second
Channel capacity	60

\*Data were determined in this investigation. All other values on this page were provided by the manufacturer.

Supply 115/230 VAC, 60 Hz.

Digital Volt Meter

Manufacturer John Fluke Mfg. Co.

Model 8000A

Supply 115 VAC/60 Hz.

Watt Meter Transducer

Manufacturer F.W. Bell, Columbus, Ohio

Model PT 2501F

Type 3 Phase, 4-Wire

Supply 120 VAC, 50/60 Hz.

Rating .60 KVA

Thermocouple Indicator

Manufacturer Doric Scientific

Model D5-350

Type J

Range 0 to 1600°F

Channel Capacity 12

Scan Manual

Supply 12 VAC, 60 Hz.

Clock

Manufacturer Dimco-Gray Co., Dayton, Ohio

Model 165

Supply 125 VAC, 60 Hz.

Variable Transformer

Manufacturer The Superior Electric Co., Bristol, Connecticut  
Type 216B  
Supply 120/240 VAC/60 Hz.  
Rating 0.98 KVA

Thermocouple Wire

Manufacturer Leeds & Northrup, Philadelphia, Pennsylvania  
Type J; Iron-constantan  
Diameter 30 gauge  
Description Enamel coating, cloth insulation

Fiberglass Insulation

Supplier Service Products, Inc., Columbus, Ohio  
Brand #703  
Dimension 2' x 4' x 2"  
Thermal Conductivity .27 BTU-in/ft-hr-°F

Heating Elements

Manufacturer Electrofilm, Inc., North Hollywood, California  
Dimension 6" x 6" x .007"  
Rating 10 watts/in<sup>2</sup>  
Brand KAPINEX  
Operating Voltage 0 to 480 AC or DC  
Operating Timetable -80°F to 500°F

Thermal Grease

Manufacturer Omega Engineering, Inc., Stamford, Connecticut

Brand	OT-201
Maximum Continuous Temperature	500°F (260°C)
Thermal Conductivity	9.6 BTU-in/hr-ft <sup>2</sup> -°F

Cooling Plate

Manufacturer	In Shop
Dimension	6" x 6" x 1"
Material	Aluminum

#### BIBLIOGRAPHY

- [1] Horvay, G., Mani, R., Veluswani, M., and Zinsmeister, G., "Transient Heat Conduction in Laminated Composites," ASME Journal of Heat Transfer, Vol. 95, 1973, p. 309.
- [2] Manaker, A., and Horvay, G., "Thermal Response of Laminated Composites," ZAMM, Vol. 55, 1975, p. 503.
- [3] Han, L. and Cosner, A., "Effective Thermal Conductivities of Fibrous Composites," ASME Journal of Heat Transfer, Vol. 103, 1981, p. 387.
- [4] Touloukian, Y., and Ho, C., editors, Thermophysical Properties of Selected Aerospace Materials, CINDAS-Purdue University, Part II, 1977, p. 180.
- [5] Larsen, D.C., "Thermal Conductivity of Boron/Epoxy, Graphite/Epoxy, ...," American Ceramic Society, Paper No. 10-C-74, 76th Annual Meeting, Chicago, Illinois.